A Network of Genes Antagonistic to the LIN-35 Retinoblastoma Protein of *Caenorhabditis elegans*

Stanley R. G. Polley and David S. Fay[1]
Department of Molecular Biology, College of Agriculture and Natural Resources, University of Wyoming, Laramie, Wyoming 82071

ABSTRACT The *Caenorhabditis elegans* pRb ortholog, LIN-35, functions in a wide range of cellular and developmental processes. This includes a role of LIN-35 in nutrient utilization by the intestine, which it carries out redundantly with SLR-2, a zinc-finger protein. This and other redundant functions of LIN-35 were identified in genetic screens for mutations that display synthetic phenotypes in conjunction with loss of *lin-35*. To explore the intestinal role of LIN-35, we conducted a genome-wide RNA-interference-feeding screen for suppressors of *lin-35*; *slr-2* early larval arrest. Of the 26 suppressors identified, 17 fall into three functional classes: (1) ribosome biogenesis genes, (2) mitochondrial prohibitins, and (3) chromatin regulators. Further characterization indicates that different categories of suppressors act through distinct molecular mechanisms. We also tested *lin-35*; *slr-2* suppressors, as well as suppressors of the synthetic multivulval phenotype, to determine the spectrum of *lin-35*-synthetic phenotypes that could be suppressed following inhibition of these genes. We identified 19 genes, most of which are evolutionarily conserved, that can suppress multiple unrelated *lin-35*-synthetic phenotypes. Our study reveals a network of genes broadly antagonistic to LIN-35 as well as genes specific to the role of LIN-35 in intestinal and vulval development. Suppressors of multiple *lin-35* phenotypes may be candidate targets for anticancer therapies. Moreover, screening for suppressors of phenotypically distinct synthetic interactions, which share a common altered gene, may prove to be a novel and effective approach for identifying genes whose activities are most directly relevant to the core functions of the shared gene.

THE retinoblastoma gene (*Rb*) was originally implicated as a tumor suppressor whose inactivation led to a rare form of pediatric eye cancer (Knudson 1971). Subsequently, loss of *Rb* function has been shown to play a causative role in the majority of known human cancers (Sherr 1996; Sherr and McCormick 2002; Viatour and Sage 2011). This observation has led to intensive studies of the pRb/p105 protein along with its family members, p107 and p130, in an effort to define the molecular and cellular functions of the pRb "pocket protein" family. Currently, the best-characterized role of pRb is as an inhibitor of cell-cycle progression. In quiescent mammalian cells, pRb family members bind to E2F-family transcription factors, leading to the repression of genes required for entry into and progression through S-phase. Transcriptional repression by pRb family members is mediated both by directly blocking the transactivation domain of activator-type E2F proteins and by the recruitment of corepressors to genomic sites bound by inhibitory-type E2Fs, leading to heterochromatin formation and maintenance (Sherr and McCormick 2002; Knudsen and Knudsen 2006; van den Heuvel and Dyson 2008; Poznic 2009; Chinnam and Goodrich 2011). In addition, many studies have focused on elucidating the network of extracellular signals and intracellular factors that regulate the phosphorylation state and activity of pRb members (Sherr and McCormick 2002; van den Heuvel and Dyson 2008; Paternot *et al.* 2010; Witkiewicz *et al.* 2011).

A growing number of studies indicate that pRb family members also regulate non-cell-cycle processes during development. pRb physically interacts with >100 putative binding partners, of which E2F family members make up only a minority (Ji and Studzinski 2004; Balciunaite *et al.* 2005; Batsche *et al.* 2005; Morris and Dyson 2001; Thomas *et al.* 2001; Chen *et al.* 2007). These include physical and functional interactions with lineage-specific transcription factors that play well-characterized roles in development, including MyoD (muscle development), Id2 (erythrocyte

Copyright © 2012 by the Genetics Society of America
doi: 10.1534/genetics.112.140152
Manuscript received February 29, 2012; accepted for publication April 19, 2012
Available freely online through the author-supported open access option.
Supporting information is available online at http://www.genetics.org/content/suppl/2012/04/27/genetics.112.140152.DC1.
[1]Corresponding author: Department of Molecular Biology, University of Wyoming, 1000 E. University Ave., Laramie, Wyoming 82071. E-mail: davidfay@uwyo.edu

production), Pdx1 (pancreas development), and C/EBP (adipocyte and monocyte differentiation) (Thomas *et al.* 2001; Rekhtman *et al.* 2003; Gery *et al.* 2004; Ji and Studzinski 2004; Lasorella *et al.* 2005; De Falco *et al.* 2006; Hua and Sarvetnick 2007; Kim *et al.* 2011). Although the majority of these proposed interactions still lack strong *in vivo* support, several have been verified in mouse models (Lasorella *et al.* 2000; Takahashi *et al.* 2004; Lasorella *et al.* 2005; Wikenheiser-Brokamp 2006; Walkley *et al.* 2008; Calo *et al.* 2010; Kim *et al.* 2011). Furthermore, in conjunction with E2F family proteins, pRb regulates many genes that have no known links to cell-cycle functions and may therefore influence a diverse range of cellular processes (Muller *et al.* 2001; Markey *et al.* 2002; Black *et al.* 2003). Finally, studies in non-mammalian systems, such as *Caenorhabditis elegans*, have identified a number of non-cell-cycle and developmental functions for the E2F-pRb network, some of which have correlates with proposed cancer-related pRb functions in mammals (van den Heuvel and Dyson 2008; Kirienko *et al.* 2010).

pRb is highly conserved across a wide range of taxa from *Caenorhabditis elegans* to mammals (Sabelli and Larkins 2006; Cao *et al.* 2010). Moreover, the pRb network in *C. elegans* is relatively simple as compared with mammals. In worms, there is only a single pRb ortholog (LIN-35), three E2F members (EFL-1, EFL-2, and F49E12.6), and one E2F dimerization partner (DPL-1) (van den Heuvel and Dyson 2008). LIN-35 was originally identified for its role in the regulation of vulval development (Ferguson and Horvitz 1989; Lu and Horvitz 1998). Interestingly, *lin-35* single mutants do not show defects in vulval development, nor is *lin-35* an essential gene under standard growth conditions. However, the combined inactivation of *lin-35* and one of several "class A" synthetic-multivulval (synMuv) genes leads to the hyper-induction of vulval tissue during hermaphrodite larval development. Control of vulval cell induction by LIN-35 is carried out in conjunction with a number of transcriptional coregulators, including the E2F ortholog, EFL-1; its dimerization partner, DPL-1; and multiple members of the conserved DREAM and NuRD complexes, whose activities mediate transcriptional repression and chromatin silencing (Lu and Horvitz 1998; Thomas and Horvitz 1999; Beitel *et al.* 2000; Ceol and Horvitz 2001; Thomas *et al.* 2003; Harrison *et al.* 2006; Andersen and Horvitz; 2007). Together, these transcriptional regulators compose the majority of "class B" synMuv genes, and animals containing mutations in both a class A and a class B synMuv gene display a characteristic Muv phenotype (Fay and Yochem 2007).

The discovery of *lin-35* as a synMuv gene marked the first non-cell-cycle function attributed to a pRb ortholog in a non-mammalian species. Since then, LIN-35 has been implicated in a number of distinct developmental and cellular processes, which include the characterization of seven *lin-35*-synthetic-lethal mutations that were identified by our laboratory through a forward genetic screen (Fay *et al.* 2002). Functions for LIN-35 identified through these screens include roles in cell-cycle regulation, pharyngeal morphogenesis, somatic gonad development, and asymmetric cell division (Fay *et al.* 2002, 2003, 2004; Bender *et al.* 2004, 2007; Cui *et al.* 2004). In addition, LIN-35 coregulates the expression of many intestinal genes with SLR-2, a C2H2-type zinc (Zn)-finger protein (Kirienko and Fay 2007; Kirienko *et al.* 2008). Whereas *lin-35* and *slr-2* single mutants develop normally, *lin-35*; *slr-2* double mutants arrest uniformly as L1 larvae because of starvation resulting from intestinal malfunction. Here we describe a genome-wide RNA interference (RNAi) screen to identify suppressors of *lin-35*; *slr-2* larval arrest. Although a majority of the RNAi clones identified specifically suppressed the *lin-35*; *slr-2* larval-arrest phenotype, a number of the clones also led to the suppression of mechanistically unrelated *lin-35*-associated phenotypes. Specifically, we identified several chromatin-modification complex members whose functions appear to antagonize many or all of the activities of LIN-35 in *C. elegans*. As these genes are highly conserved, they may represent targets that could be exploited to neutralize the deleterious effects of pRb loss in mammals.

Materials and Methods

Strains

Nematodes were handled according to standard protocols (Stiernagle 2006). Animals were maintained at 20° unless otherwise stated. The following strains were used in this study: wild-type N2 (Bristol), *lin-35(n745)*, MH1620 [*lin-35(n745)*; *slr-2(ku297)*; *kuEx119*], WY617 [*dpl-1 (n2994)*; *slr-2*; *kuEx119*], WY83 [*lin-35*; *ubc-18(ku354)*; *kuEx119*], MH1621 [*lin-35*; *fzr-1(ku298)*; *kuEx119*], WY251[*lin-35*; *spr-1(ar205)*; *kuEx119*], WY119 [*lin-35*; *pha-1(fd1)*; *kuEx119*], WY142 [*xnp-1(fd2) lin-35*; *kuEx119*], JD118 [*inx-6(rr5)*], AA790 [*lin-15AB (n765)*], WY758 [*lin-35 unc-13*; *npp-5*; *kuEx119*], WY761 [*lin-35 unc-13*; *hcf-1*; *kuEx119*], WY760 [*lin-35 unc-13*; *wdr-5.1*; *kuEx119*], RB777 [*hcf-1(ok559)*], VC1494 [*npp-5 (ok1966)*], RB1304 [*wdr-5.1 (ok1417)*], and JM63 [*elt-2*::GFP]. *kuEx119* is an extrachromosomal array containing wild-type copies of *lin-35* along with the SUR-5::GFP reporter (Gu *et al.* 1998; Fay *et al.* 2002).

RNAi screening and quantification of lin-35; slr-2 suppression

RNAi feeding screens were performed using the Geneservice RNAi library (Kamath *et al.* 2003), following standard protocols (Timmons 2006). Four or five *lin-35*; *slr-2*; *kuEx119* L4 larvae were transferred to individual RNAi feeding plates, incubated at 20° for 3 days, and then qualitatively assessed for escape of L1 arrest in *kuEx119*-minus (GFP–) F_1 progeny. Putative suppressors were retested by placing 15–20 L4 larvae on RNAi feeding plates for 12 hr and then transferring adults to fresh RNAi plates for 12 additional hours, after which adults were removed and total embryos were counted. *kuEx119*-positive (GFP+) F_1 progeny were then removed every 12 hr and counted. After 4 days, the

number of larvae developing beyond the L1 arrest stage were counted and divided by the calculated total number of *kuEx119*-negative (GFP–) F_1 progeny. For statistical analysis, the experiments were repeated five times and numbers were pooled. A Fisher's exact test was performed for each suppressor clone to assign significance using a *P*-value cutoff of 0.001. Suppressor clones were also sequenced to determine their correct identity.

inx-6 starvation arrest assay

inx-6(rr5ts) mutants arrest because of foregut defects that result in starvation at the nonpermissive temperature of 25° (Li *et al.* 2003). Twenty-five to 30 L4 *inx-6* mutants were initially placed on vector-control (pPD129.36) or suppressor RNAi plates at 15°. Adult worms were transferred to corresponding RNAi plates 12 hr later and allowed to lay embryos for 3 hr. Total embryos (TEs) were counted and then allowed to develop at 15° for either 16 or 24 hr, at which time they were shifted to 25°. Plates were then kept at 25° for 4–5 days, and adult worms (AWs) were then counted. The percentage of adult worms was calculated as (AWs/TEs) × 100.

Oil Red O staining

Oil Red O staining was conducted as described but without the freeze–thaw steps (O'Rourke *et al.* 2009; Soukas *et al.* 2009). *lin-35*; *slr-2*; *kuEx119* L4 larvae were placed on vector-control or suppressor RNAi feeding plates and allowed to develop into adults. Adult worms were bleached, and their liberated embryos were washed, transferred to corresponding RNAi plates, and allowed to develop to roughly synchronized L1 larvae, as monitored by an L1 apoptotic event in their tails (T.ppp) (Sulston and Horvitz 1977). Animals were mounted and images of *kuEx119*-minus (GFP–) larvae were captured.

Cycloheximide and geneticin (G418) assays

Cycloheximide dilutions were combined with cultured OP_{50} bacteria and allowed to dry on NGM plates. For G418-containing plates, G418 dilutions were added to NGM medium prior to pouring. Fifteen to 20 L4 *lin-35*; *slr-2*; *kuEx119* or *dpl-1*; *slr-2*; *kuEx119* worms were placed on plates and allowed to develop into adults. Adults were then transferred to identically treated plates and allowed to lay embryos for 4–5 hr, after which adults were removed and TEs were counted. *kuEx119*-postive (GFP+) worms (GWs) were removed and counted every 12 hr. After 3–4 days, the number of *kuEx119*-negative (GFP–) worms (*i.e.*, suppressed worms, or SWs) that developed past the L1 arrest stage were counted, and the percentage suppression (S%) was calculated using the formula S% = [SWs/(TEs − GWs)] × 100.

Intestinal and distal tip cell hyper-proliferation assays

Intestinal hyper-proliferation was assayed using strains carrying an *elt-2*::*GFP* reporter (Fukushige *et al.* 1998). *fzr-1(ku298)*; *elt-2*::*GFP* L4 larvae were placed on RNAi feeding plates for *lin-35*, vector-control, or double RNAi combinations of *lin-35* and one of the suppressors. All double-RNAi experiments were controlled for optical density such that a 1:1 ratio of each bacterial solution was used at the time of plate seeding. Intestinal nuclei were counted using standard fluorescence and DIC optics. Distal tip cell (DTC) hyper-proliferation was assessed on the basis of gonad arm bifurcations in *kuEx119*-minus (GFP–) young adult progeny of *lin-35*; *fzr-1*; *kuEx119* mutants grown on either vector-control or suppressor RNAi feeding plates.

High-temperature arrest assay

lin-35(n745) L4 larvae were transferred to vector-control or suppressor RNAi plates and incubated at 26°. Adult worms were then transferred to corresponding RNAi plates and allowed to lay embryos for 5 hr at 26°. Adults were removed and embryos were counted. After 2–3 days, larvae that had developed beyond the L1 arrest stage were counted and divided by the total number of embryos to calculate the percentage suppression.

Results

A genome-wide RNAi screen for suppressors of lin-35; slr-2 larval arrest

lin-35; *slr-2* double mutants exhibit a nearly uniform arrest as L1 larvae because of defects in nutrient utilization (Kirienko *et al.* 2008). Homozygous *lin-35*; *slr-2* double mutants, however, can be maintained by the presence of an extrachromosomal array (*kuEx119*) that contains *lin-35*-rescuing sequences as well as a ubiquitously expressed SUR-5::GFP reporter (Fay *et al.* 2002). Because extrachromosomal arrays are meiotically unstable, array-positive hermaphrodites fail to segregate the array to all of their self-progeny (Mello *et al.* 1991). In the case of *lin-35*; *slr-2*; *kuEx119*, ∼30% of self-progeny fail to inherit the array and can be easily identified as L1-arrested larvae that lack GFP expression (Kirienko *et al.* 2008).

To identify suppressors of *lin-35*; *slr-2* larval arrest, we carried out a genome-wide RNAi feeding screen using the GeneService library (Timmons *et al.* 2001; Kamath *et al.* 2003). Positive RNAi clones were identified by an increase in the proportion of GFP– self-progeny that developed past the L1 stage. Of the 16,757 genes represented in the RNAi feeding library, 26 suppressors were identified (0.16% of total clones screened). RNAi clones were sequence verified, and suppression by each clone was tested in five independent trials and shown to be statistically significant ($P <$ 0.001, Fisher's exact test; Figure 1A). We also confirmed suppression using genetic mutants for three of the identified suppressors: *npp-5* (*ok1966*), *hcf-1* (*ok559*), and *wdr-5.1 (ok1417)* (Figure 1, B–D). Confirmation by genetic mutations, as well as the relatively low frequency of positive clones, indicates that our RNAi screening approach yielded results that were both reproducible and specific.

There was considerable variability among the RNAi clones with respect to the percentage of suppressed animals as well as the terminal developmental stage to which *lin-35*;

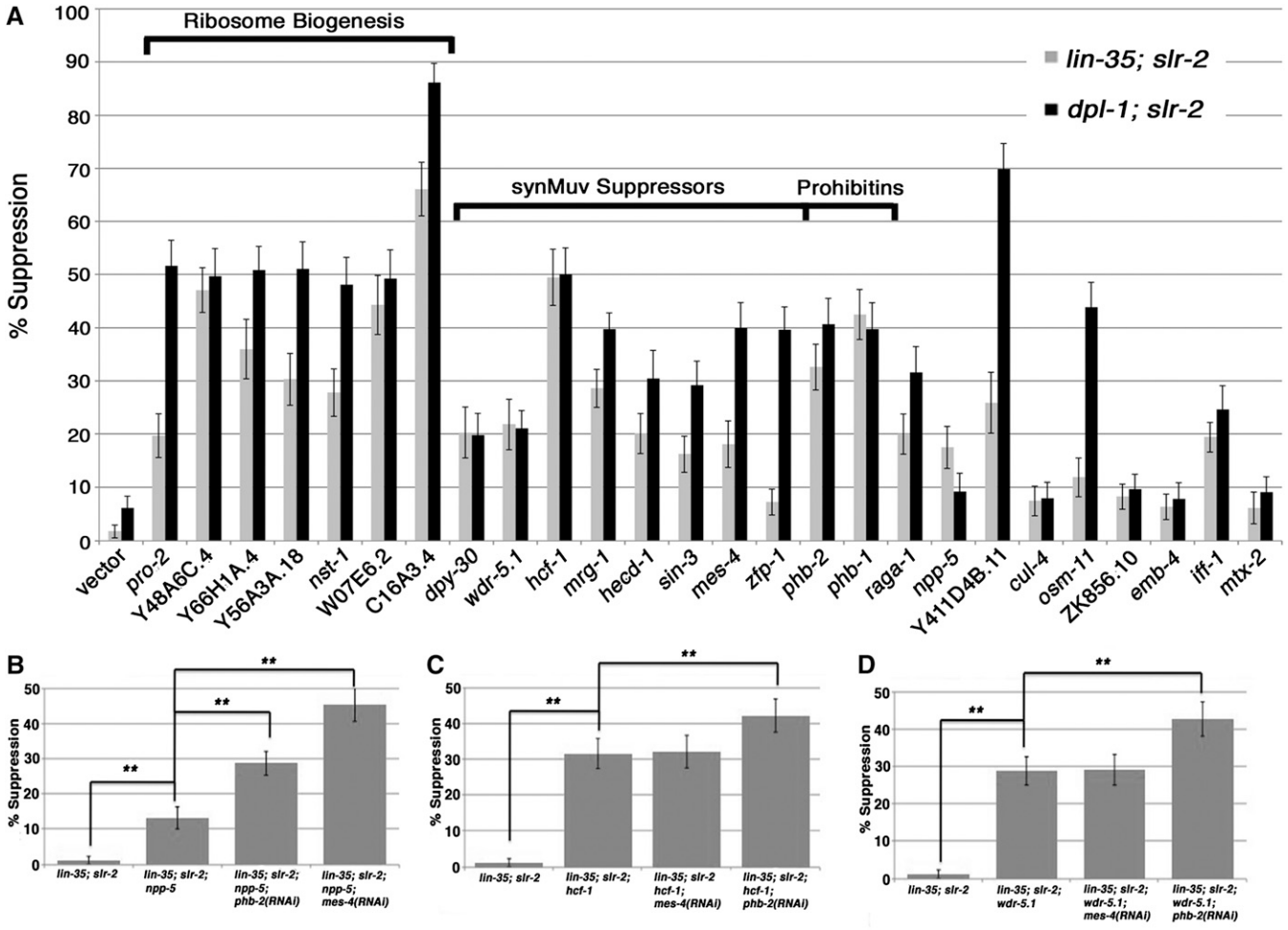

Figure 1 Suppressors of *lin-35*; *slr-2* and *dpl-1*; *slr-2* L1 larval arrest. (A) Percentage suppression of larval arrest by 26 sequence-confirmed RNAi clones. Vector denotes a control RNAi. Suppressors have been organized into functional classes. Suppression of L1 arrest using genetic mutations was also assayed in (B) *lin-35*; *npp-5*; *slr-2* triple mutants, (C) *lin-35*; *hcf-1*; *slr-2* triple mutants, and (D) *lin-35*; *wdr-5.1*; *slr-2* triple mutants. In addition, RNAi of several *lin-35*; *slr-2* suppressors was carried out on the indicated genotypes to test for further enhancement of suppression (B–D). Error bars represent 95% confidence intervals. In A, all *P*-values were <0.001 except for *dpl-1*; *slr-2* mutants on RNAi plates corresponding to *cul-4*, ZK856.10, *emb-4*, and *mtx-2*. In B–D, double asterisks indicate $P < 0.01$.

slr-2 animals progressed (supporting information, Figure S1; Table S1). For example, *lin-35*; *slr-2* mutants treated with RNAi for *hcf-1*, *mes-4*, *mrg-1*, *sin-3*, *hecd-1*, or *raga-1* were able to develop into fertile adults, whereas other RNAi clones resulted in sterility or arrest prior to adulthood. In fact, several of the strongest suppressors (*e.g.*, C16A3.4, Y48A6C.4, *phb-1*, and *phb-2*) lead to arrest as sterile adults. In a number of cases, the identified suppressor genes have previously been shown to be required for late larval development or fertility, thereby precluding suppression to viable or fertile adults (Table S1) (Hanazawa *et al.* 2004; Checchi and Kelly 2006; Voutev *et al.* 2006; Rodenas *et al.* 2009).

Previous studies found *slr-2* to be synthetically lethal with *dpl-1*, which encodes the sole E2F dimerization partner homolog in *C. elegans* and regulates transcription through its interaction with E2F family members (Ceol and Horvitz 2001; Page *et al.* 2001; Kirienko *et al.* 2008). The *dpl-1*; *slr-2* arrest phenotype is morphologically indistinguishable from that of *lin-35*; *slr-2* mutants, although the penetrance of L1 arrest is somewhat weaker: 93.9% for *dpl-1*; *slr-2* mutants *vs.* 98.2% for *lin-35*; *slr-2* mutants. We found that all but four of the *lin-35*; *slr-2* suppressors also significantly suppress the *dpl-1*; *slr-2* arrest phenotype (Figure 1A). In most cases, the percentage of suppressed animals was greater than that observed for *lin-35*; *slr-2*, which correlates with the slightly less penetrant phenotype of *dpl-1*; *slr-2* mutants. The ability of the RNAi clones to suppress both *lin-35*; *slr-2* and *dpl-1*; *slr-2* mutants suggests that the RNAi clones correct an underlying defect that is shared in both double mutants (Kirienko *et al.* 2008). It also argues that suppression by the RNAi clones is not informational or due to the specific nature of the *lin-35(n745)* (opal stop) or *dpl-1* (n2994) (splice acceptor site mutation) genetic lesions. Because the phenotypes of *lin-35*; *slr-2* and *dpl-1*; *slr-2* mutants are very similar, the majority of our experiments were carried out using *lin-35*; *slr-2* mutants only.

Table 1 *lin-35; slr-2* suppressor identities

Genes sorted by category	Relevant ortholog/*C. elegans* functions/InterPro domain predictions
Ribosome biogenesis	
pro-2	Yeast ribosome maturation and intranuclear transport protein, Noc2/ribosome biogenesis, germline development/novel
nst-1	Human GNL3L nucleostemin family member highly expressed in embryonic stem cells/germ cell proliferation/GTP binding domain
Y48A6C.4	Yeast Ipi1/germline proliferation, ribosome biogenesis/ribosome biogenesis, germline development/ armadillo-like helix
Y56A3A.18	Yeast Bud20/ribosome biogenesis, germline development/zinc-finger C2H2
Y66H1A.4	Yeast nucleolar ribonucleoprotein H/ACA snoRNP complex member Gar1/pre-rRNA processing, telomere maintenance/novel
W07E6.2	Yeast rRNA processing and intranuclear transport of 60S ribosomal subunit Rsa4/ribosome biogenesis/WD40
C16A3.4	Human ZF622/unknown function/zinc-finger C2H2
Mitochondrial prohibitins	
phb-1	Human PHB1/mitochondrial morphology, mitochondrial membrane potential, fat utilization repression/prohibitin
phb-2	Human PHB2/mitochondrial morphology, mitochondrial membrane potential, fat utilization repression/prohibitin
synMuv suppressors	
hcf-1	Human host cell factor C1, methyltransferase complex member/life span as a DAF-16 regulator, histone modification/fibronectin III-like domain
mes-4	Yeast Set2/Set1 H3K4-like methyltransferase, transcriptional activation of autosomes, dosage compensation/SET domain, zinc-finger ring type
mrg-1	Human TF MRG15/PGC survival, autosome associated, transcriptional regulator of germ and somatic tissue/chromodomain
wdr-5.1	Yeast Set1 H3K4 methyltransferase-like complex member Swd3/life span, nuclear localization/WD40 repeat
hecd-1	Yeast E3 ubiquitin ligase Ufd4/E3 ubiquitin ligase/ankyrin repeat, galactose-binding domain
dpy-30	Human Set1 H3K4 methyltransferase interacting member DPY30/SDC complex member, NOX-1 complex member/novel
sin-3	Yeast histone deacetylase Sin3/histone-silencing deacetylase, male development/glutamine + asparagine-rich domain, PAH domain
zfp-1	Human AF-10/RNAi, gene silencing/leucine zipper, zinc-finger PHD type
Other	
raga-1	Human Ras-related GTPase RagA and RagB/Rag GTPase, life span, TOR pathway regulator/novel
npp-5	Human Nup107/nuclear pore complex member, nuclear assembly/novel
Y41D4B.11	Yeast mannosylphosphate transferase Mnn6/unknown function/novel
cul-4	Yeast Cul3/ubiquitin ligase, genome stability, DNA replication/winged helix-turn-helix transcriptional repressor DNA-binding domain
osm-11	Nematode-specific/osmosensation, osmotic resistance, defecation rhythm/novel
ZK856.10	Yeast RNA polymerase III complex member Rpc25/unknown function/novel
emb-4	Human AQR/IBP160/germline chromatin condensation, embryonic development/ATPase
iff-1	Yeast translation elongation factor eIF-5A/P granule component localization, germ-cell proliferation/novel
mtx-2	Human metaxin-2/unknown function/novel

Suppressors of lin-35; slr-2 fall into several functional categories

Seventeen of the 26 suppressors identified from the *lin-35*; *slr-2* screen can be placed into three functional classes: (1) ribosome biogenesis genes, (2) mitochondrial prohibitins, and (3) synMuv suppressors (Figure 1A; Table 1). The remaining 9 genes vary broadly in function but include several of the strongest suppressors (Figure 1A). A more detailed description of these genes, along with insights into their means of suppression, is discussed below. To functionally examine the suppressor classes, we placed *lin-35*; *slr-2*; *sup* triple mutants (where "*sup*" refers to one of the isolated suppressors) on RNAi plates targeting suppressors in either the same or a different class. In the case of the three synMuv suppressor genes *hcf-1*, *mes-4*, and *wdr-5.1*, no increase in suppression was observed when these genes were combinatorially inactivated *vs.* single-gene inhibition (Figure 1, B–D). This lack of an additive effect is consistent with their gene products acting within a single methyltransferase complex (Table 1) (Dehe and Geli 2006; Wu *et al.* 2008). In addition, no enhancement of *lin-35*; *slr-2* suppression was observed following double RNAi of the two prohibitin-binding partners *phb-1* and *phb-2* relative to RNAi of either clone individually (data not shown). Conversely, additive suppression was observed in *lin-35*; *slr-2* triple mutants with *npp-5*, *hcf-1*, and *wdr-5.1* following RNAi of *phb-2* and in *lin-35*; *slr-2*; *npp-5* triple mutants treated with *mes-4(RNAi)* (Figure 1, B–D). Taken together, these findings are consistent with different gene classes acting through distinct mechanisms to suppress *lin-35*; *slr-2* larval arrest.

Ribosome biogenesis genes

Seven genes implicated in ribosome biogenesis were isolated from the genome-wide screen (Figure 1A; Table 1).

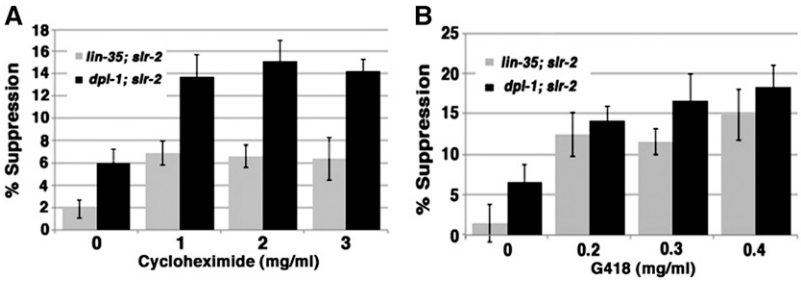

Figure 2 Chemical inhibition of protein translation suppresses *lin-35*; *slr-2* and *dpl-1*; *slr-2* double mutants. (A) Cycloheximide and (B) G418 treatments significantly suppress L1 larval arrest of *lin-35*; *slr-2* and *dpl-1*; *slr-2* strains as compared with the no-treatment controls ($P < 0.001$). Error bars represent 95% confidence intervals.

For this class, which includes *pro-2*, suppressed *lin-35*; *slr-2* mutants arrested as sterile adults (Figure S1). The roles of these genes in ribosome biogenesis are inferred both from sequence homology to well-characterized orthologs in yeast and from studies in *C. elegans* showing that mutations in a subset of these genes lead to defects in rRNA processing (Bousquet-Antonelli *et al.* 2000; Vanrobays *et al.* 2001; Galani *et al.* 2004; Voutev *et al.* 2006). In yeast, Gar1/Y66H1A.4 and Ipi1/Y48A6C.4 are required for 18s and 35s pre-rRNA processing, respectively (Krogan *et al.* 2004), whereas orthologs of *nst-1*, *pro-2*, and W07E6.2 have demonstrated roles in the transport of pre-ribosomal subunits (Bassler *et al.* 2001; Milkereit *et al.* 2001; de la Cruz *et al.* 2005). Notably, worms with mutations in five of these genes (*nst-1*, *pro-2*, W07E6.2, Y56A3A.18, and Y48A6C.4) form proximal germline tumors resulting from defects in the developing somatic gonad (Killian and Hubbard 2004; Voutev *et al.* 2006).

The strongest suppressor identified by our screen, C16A3.4, may also act through the ribosome biogenesis pathway. In yeast, Rei1/C16A3.4 has defined roles in 60S ribosomal subunit maturation and subsequent recycling of subunit shuttle members (Albanese *et al.* 2010; Lo *et al.* 2010). Similar to other ribosome biogenesis suppressors, RNAi of C16A3.4 caused sterility in both N2 and suppressed *lin-35*; *slr-2* backgrounds. Unlike other ribosome biogenesis genes, however, RNAi of C16A3.4 did not induce proximal germline tumors (data not shown), and C16A3.4 contains multiple C2H2 Zn-finger domains, suggesting a possible role in transcriptional regulation. Interestingly, the human ortholog of C16A3.4, ZNF622, has been proposed to be a transcriptional regulator of intestinal genes and is overexpressed in colorectal tumors (Kleivi *et al.* 2007). Several additional suppressors may also act through translational regulation mechanisms. ZK856.10 encodes a putative ortholog of Rpc25, a subunit of RNA polymerase III, which is required for the transcription of small RNAs including tRNAs and the 5S rRNA (Zaros and Thuriaux 2005). In addition, *iff-1* encodes a protein with homology to EIF5A, a conserved protein with suggested roles in protein translation (Zanelli and Valentini 2007).

Previous work in our laboratory demonstrated that *lin-35* and *slr-2* coregulate a large number of intestinal genes and that genes upregulated in single mutants are in many cases synergistically misregulated in *lin-35*; *slr-2* and *dpl-1*; *slr-2* double mutants (Kirienko *et al.* 2008). We therefore postulated that suppression of larval arrest by inhibition of ribosome biogenesis might reduce the translation of intestinal mRNAs that are deleterious when overexpressed. To test this model, we asked whether two well-characterized inhibitors of protein translation, cycloheximide and G418, could suppress *lin-35*; *slr-2* and *dpl-1*; *slr-2* larval arrest. Although toxicity was evident with these drugs, *lin-35*; *slr-2* and *dpl-1*; *slr-2* strains showed significant suppression of L1 arrest when grown on sublethal concentrations of either compound (Figure 2). Thus, a net reduction in protein translation may reduce the levels of misexpressed intestinal proteins in *lin-35*; *slr-2* and *dpl-2 slr-2* mutants, such that their negative impact on intestinal functions is diminished. At present we have no direct evidence to indicate whether translational inhibition of one or multiple targets of LIN-35 and SLR-2 is required to achieve suppression. However, the absence of intestinal targets of LIN-35 and SLR-2 from the suppressor screen suggests that a reduction in the expression of individual targets may not be sufficient to achieve suppression.

Mitochondrial prohibitins

Two genes identified by our screen, *phb-1* and *phb-2*, encode orthologs of the mitochondrial prohibitins (Figure 1A; Table 1). PHB1 and PHB2 are structurally related proteins that are highly conserved from yeast to humans. PHB1 and PHB2 form large megadalton complexes within the inner mitochondrial membrane where they are thought to regulate mitochondrial morphology and maintain membrane potential (Artal-Sanz and Tavernarakis 2009a,b; Osman *et al.* 2009; Van Aken *et al.* 2010). Work in several organisms further indicates that prohibitins also reside in the nucleus where they may control transcription through a number of distinct mechanisms (Mishra *et al.* 2006, 2010). We identified an RNAi clone corresponding to *phb-2* as a strong suppressor of *lin-35*; *slr-2* arrest (32.2%; Figure 1). *lin-35*; *slr-2*; *phb-2(RNAi)* mutants arrested as sterile adults, an outcome consistent with *phb-2(RNAi)* inducing sterility in wild type (Kamath *et al.* 2003; Rual *et al.* 2004). We also generated a *phb-1(RNAi)* feeding construct and observed strong suppression of *lin-35*; *slr-2* (41.9%). As noted above, double RNAi of *phb-1* and *phb-2* conferred no additive suppression, consistent with both proteins acting as partners within a complex. Interestingly, mammalian PHB1 and PHB2 physically interact with all three mammalian pRb family proteins as well as E2F (Wang *et al.* 1999a,b, 2002; Fusaro *et al.* 2002). However, given that the mammalian prohibitins are thought to repress E2F target-gene expression in a pRb-

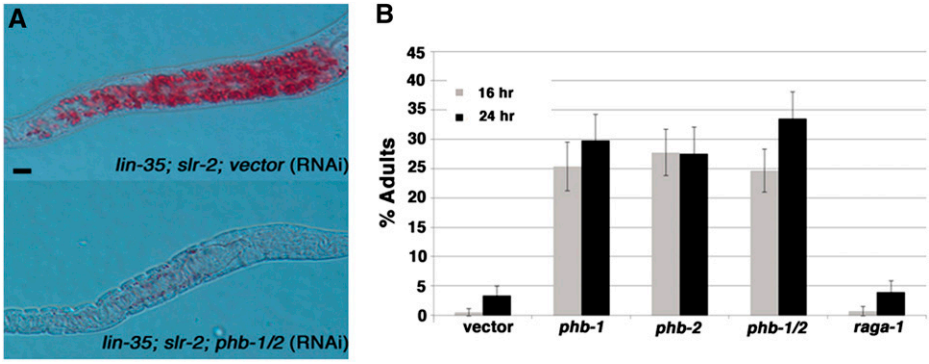

Figure 3 Analysis of suppression by mitochondrial prohibitins. (A) Oil Red O staining, which detects fat, is markedly reduced in *lin-35*; *slr-2* L1 larvae treated with *phb-1/2 (RNAi) vs.* control RNAi. Bar, 10 μm. (B) Suppression of larval arrest in *inx-6* feeding-defective mutants following RNAi of the prohibitins. Temperature-sensitive *inx-6 (rr5ts)* mutants were grown on RNAi plates at 15° for 16 or 24 hr before up-shift to 25°. Error bars represent 95% confidence intervals. For all treatment concentrations relative to vector control, $P < 0.01$, except for *raga-1*.

dependent manner, their loss would not be expected to compensate for pRb inactivation. This suggests that suppression of *lin-35*; *slr-2* and *dpl-1*; *slr-2* by *phb-1* and *phb-2* occurs through a mechanism that does not involve direct interactions with *C. elegans* pRb or E2F family members. However, it is also possible that LIN-35 does bind to *C. elegans* prohibitin members and that their regulatory relationship is different from that described in mammals.

In aging wild-type adult worms, RNAi of *phb-1* and *phb-2* leads to a strong reduction in intestinal fat stores (Artal-Sanz and Tavernarakis 2009b, 2010). Given that *lin-35*; *slr-2* mutants arrest because of a defect in nutrient utilization, we tested whether prohibitin knockdown could also alter fat storage at the L1 stage of arrest. Notably, *lin-35*; *slr-2* treated with RNAi of *phb-1* or *phb-2* showed a dramatic decrease in L1 fat stores based on staining with Oil Red O (Figure 3A). This decrease in fat stores at the L1 stage suggests a mechanism for suppression by the prohibitins. Namely, utilization of fat reserves in nutrient-deprived *lin-35*; *slr-2* mutants may allow these animals to bypass the L1 diapause developmental arrest that is normally initiated under conditions of starvation (Fukuyama *et al.* 2006; Kirienko *et al.* 2008). Thus, L1 arrest in *lin-35*; *slr-2* mutants is likely not due to a complete failure of the intestine to process nutrients but may result from a reduction in metabolic capacity that falls below a set threshold, thereby activating a nutrient-sensing developmental checkpoint.

To test our model, we asked whether prohibitin knockdown was capable of suppressing starvation-induced L1 arrest in an independent genetic background. INX-6 is required for pharyngeal gap junction formation and muscle contractions that are necessary for feeding (Li *et al.* 2003). Temperature-sensitive *inx-6(rr5ts)* mutants are viable at 15° but arrest uniformly as L1 larvae at 25° because of starvation (Li *et al.* 2003). A series of temperature-shift experiments was carried out in which *inx-6(rr5ts)* embryos were incubated at 15° for either 16 or 24 hr, at which point animals were late-stage embryos or L1 larvae. Plates were then transferred to 25° for the remainder of development. *inx-6* mutants grown on vector RNAi plates rarely developed to adulthood after temperature up-shift at either 16 or 24 hr (Figure 3B). In contrast, *inx-6* mutants grown on *phb-1*, *phb-2*, or *phb-1/2* RNAi plates showed a >10-fold increase in the percentage of worms that reach adulthood (Figure 3B). In addition, *inx-6* mutants treated with *phb-1* or *phb-2* RNAi showed reduced levels of L1 fat stores on the basis of Oil Red O staining, consistent with effects observed for *lin-35*; *slr-2* larvae (data not shown). The ability of *phb-1* and *phb-2* to suppress the mechanistically disparate phenotypes of *inx-6* and *lin-35*; *slr-2* mutants indicates that the loss of prohibitins leads to suppression of starvation-induced L1 arrest through the utilization of normally unavailable fat stores. In addition, we tested the other 24 *lin-35*; *slr-2* suppressors identified from our screen for fat storage defects and *inx-6* suppression, including *raga-1*, a GTPase target of the nutrient-responsive TOR pathway (Figure 3B and data not shown) (Schreiber *et al.* 2010). These tests failed to identify other similarly acting suppressors, indicating that the prohibitins act through a unique mechanism of bypass suppression.

synMuv suppressors

Among the 26 *lin-35*; *slr-2* suppressor genes, 8 were previously shown to suppress the synMuv phenotype of *lin-15AB(n765)* mutants (Table 1) (Andersen *et al.* 2006; Cui *et al.* 2006). This class of genes consists primarily of transcriptional regulators, including a number of chromatin-modifying factors. Homologs of proteins encoded by *mes-4*, *hcf-1*, *wdr-5.1*, and *dpy-30* are components of the set1/COMPASS histone H3K4 methylation complex, suggesting that they may act within a similar complex in *C. elegans* (Xu and Strome 2001; Wysocka *et al.* 2003; Bender *et al.* 2006; Simonet *et al.* 2007; Halbach *et al.* 2009; Murton *et al.* 2010; Li and Kelly 2011). However, although homologous to the Set1 component of the Set1/COMPASS complex, studies in *C. elegans* suggest that MES-4 acts primarily as an autosome-specific H3K36 methyltransferase (Furuhashi *et al.* 2010; Rechtsteiner *et al.* 2010). MRG-1 is a member of the NuA4 complex, which promotes acetylation of histone H4 and subsequent exchange with the Htz histone variant (Eisen *et al.* 2001; Takasaki *et al.* 2007). The remaining three synMuv suppressor genes and their orthologs in other systems are more poorly characterized at a functional level; proteins encoded by *hecd-1*, *sin-3*, and *zfp-1* are homolgous to the yeast Ufd4 ubiquitin ligase (Xie and Varshavsky 2000), the Sin3 histone deacetylase (Bernstein *et al.* 2000;

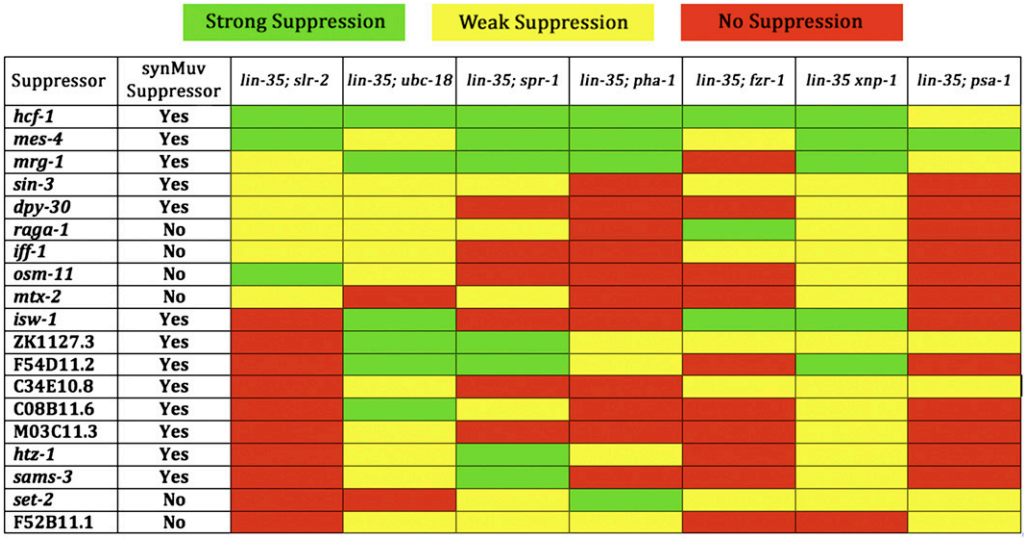

Suppressor	synMuv Suppressor	*lin-35; slr-2*	*lin-35; ubc-18*	*lin-35; spr-1*	*lin-35; pha-1*	*lin-35; fzr-1*	*lin-35 xnp-1*	*lin-35; psa-1*
hcf-1	Yes							
mes-4	Yes							
mrg-1	Yes							
sin-3	Yes							
dpy-30	Yes							
raga-1	No							
iff-1	No							
osm-11	No							
mtx-2	No							
isw-1	Yes							
ZK1127.3	Yes							
F54D11.2	Yes							
C34E10.8	Yes							
C08B11.6	Yes							
M03C11.3	Yes							
htz-1	Yes							
sams-3	Yes							
set-2	No							
F52B11.1	No							

Figure 4 Suppressors of multiple *lin-35*-synthetic phenotypes. Suppression by RNAi clones (leftmost column) of the indicated genotypes (top row) was scored as negative (red), moderate (yellow: 10–30% suppression), and strong (green: 30–100% suppression). All suppression values are normalized to the vector control RNAi values for each given genotype. For suppression values, see Figure S2, Figure S3, Figure S4, Figure S5, Figure S6, Figure S7, and Figure S8.

Silverstein and Ekwall 2005), and the Nto1 histone acetyltransferase complex member, respectively (Shi *et al.* 2007; Hang and Smith 2011).

Given that about one-third of the identified *lin-35*; *slr-2* suppressors were previously shown to suppress the *lin-15ab* synMuv phenotype, we tested the remaining *lin-35*; *slr-2* suppressors by RNAi to see if they, too, could suppress synMuv. None of the remaining suppressors were capable of suppressing the *lin-15ab* synMuv phenotype (Figure S2), consistent with their absence from the published genome-wide RNAi screen (Cui *et al.* 2006). Furthermore, we verified that all eight of the synMuv suppressors identified by our screen suppressed the synMuv phenotype (data not shown), indicating that our assay for synMuv suppression was robust. Finally, we tested 24 additional synMuv suppressors isolated by Cui and colleagues to see if these could suppress the *lin-35*; *slr-2* phenotype (Table S2). None of these RNAi clones suppressed *lin-35*; *slr-2* (data not shown). Thus, although there is clear overlap between the genes identified as *lin-35*; *slr-2* and synMuv suppressors, these results suggest that the majority of suppressors within each class act through mechanisms that are specific to the individual phenotypes.

Suppression of multiple lin-35-associated phenotypes by a subset of lin-35; slr-2 suppressors

We next decided to test all 26 *lin-35*; *slr-2* suppressors for suppression of six independent *lin-35*-synthetic genotypes previously characterized in our laboratory. These include (1) *lin-35*; *fzr-1*, which shows defects in cell-cycle regulation (Fay *et al.* 2002); (2) *lin-35*; *ubc-18* and *lin-35*; *pha-1*, which are defective at pharyngeal morphogenesis (Fay *et al.* 2003, 2004; Qiu and Fay 2006; Mani and Fay 2009); (3) *lin-35*; *spr-1* and *lin-35*; *xnp-1*, which are defective at somatic gonad and germline development (Bender *et al.* 2004, 2007); and (5) *lin-35*; *psa-1*, which arrests as larvae and is defective at asymmetric cell division (Cui *et al.* 2004). Notably, of the 26 *lin-35*; *slr-2* suppressors, 9 suppressed multiple *lin-35*-synthetic phenotypes (Figure 4; Figure S3, Figure S4, Figure S5, Figure S6, Figure S7, and Figure S8). These multiphenotypic *lin-35* suppressors included five synMuv suppressors as well as four *lin-35*; *slr-2* suppressors that did not suppress the synMuv phenotype. We also tested the 24 synMuv suppressors that failed to suppress *lin-35*; *slr-2* and found that 8 of them were capable of suppressing multiple *lin-35*-synthetic phenotypes (Figure 4; Figure S3, Figure S4, Figure S5, Figure S6, Figure S7, and Figure S8; Table S2). In total, we identified 19 RNAi clones that suppress multiple *lin-35*-synthetic phenotypes.

Notably strong suppressors were *hcf-1*, *mes-4*, and *mrg-1*, which suppressed nearly all *lin-35*-synthetic phenotypes. These findings suggest that these conserved chromatin modification factors regulate, directly or indirectly, the same core targets as LIN-35 and that their normal function is antagonistic to that of LIN-35. Also among the strongest suppressors were *isw-1*, *htz-1*, ZK1127, and F54D11.2, none of which significantly suppressed *lin-35*; *slr-2* mutants. Given that *hcf-1* and *mes-4* encode homologs of Set1/COMPASS H3K4 methyltransferase complex members, we tested nine additional putative complex members for their ability to suppress *lin-35*-synthetic phenotypes. Notably, the H3K4 methyltransferase, *set-2*, and the yeast Cps40 homolog, F52B11.1, suppressed multiple phenotypes. (Figure 4, Figure S3, Figure S4, Figure S5, Figure S6, Figure S7, and Figure S8). Consistent with our genome-wide screen, however, RNAi of these genes did not suppress *lin-35*; *slr-2*. Interestingly, several of these multi-phenotypic *lin-35* suppressors are not known to regulate chromatin, including *raga-1*, a target of TOR signaling (Schreiber *et al.* 2010), and *osm-11*, an osmosensation factor with suggested roles in Notch signaling (Wheeler and Thomas 2006; Komatsu *et al.* 2008).

Of particular interest to us were eight suppressors of *lin-35*; *fzr-1* embryonic lethality (Figure 4; Figure S3). To examine these suppressors in more detail, we assayed proliferation of two cell types known to undergo excess

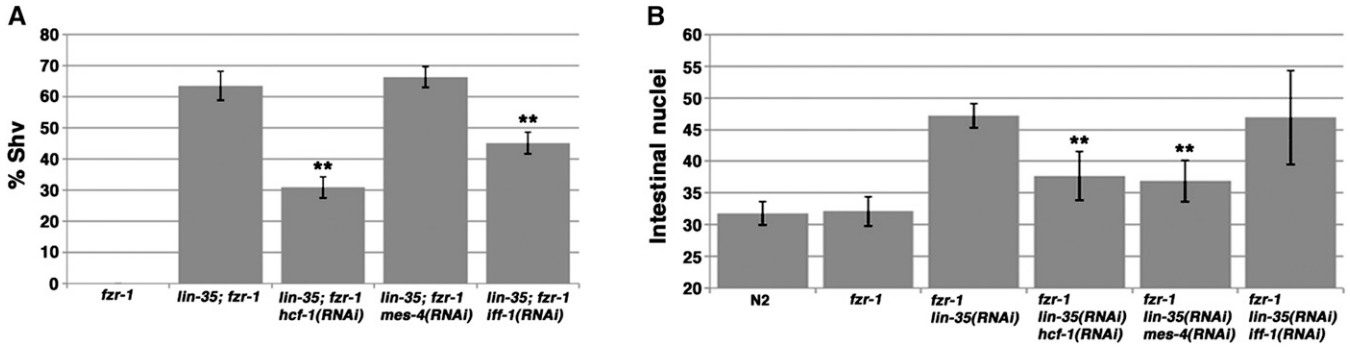

Figure 5 Suppression of *lin-35*; *fzr-1* hyper-proliferation defects. (A) Percentage of adult animals that display a Shv phenotype, which results from excess divisions of the DTCs. Whereas RNAi of *hcf-1* and *iff-1* significantly suppresses ectopic divisions of the DTCs, *mes-4(RNAi)* failed to do so. (B) Number of intestinal cell nuclei as judged by an *elt-2*::GFP reporter. RNAi of *hcf-1* and *mes-4* significantly suppresses the intestinal cell hyper-proliferation defect of *lin-35*; *fzr-1* mutants. Error bars represent 95% confidence intervals. $^{**}P < 0.01$.

divisions in *lin-35*; *fzr-1* mutant larvae (Fay *et al.* 2002). We found that, among the *lin-35*; *fzr-1* suppressors, only *hcf-1* RNAi and *iff-1* RNAi inhibited extra divisions of the DTCs (the Shv phenotype) in *lin-35*; *fzr-1* mutants (Figure 5A). The presence of at least one DTC per gonad arm in *lin-35*; *fzr-1* mutants treated with *hcf-1* or *iff-1* RNAi indicates that inhibition of these genes does not prevent DTC differentiation *per se*. Furthermore, our previous studies indicate that the extra DTCs present in *lin-35*; *fzr-1* gonads are derived from a single precursor DTC in each arm and are not due to mis-specification of the DTC fate by other cell types (Fay *et al.* 2002). We also observed that RNAi of *hcf-1* or *mes-4* suppressed ectopic intestinal cell divisions (Figure 5B). The inability of other suppressors of *lin-35*; *fzr-1* embryonic arrest to significantly reduce excess cell divisions during postembryonic development may reflect a lack of sensitivity in these particular assays or possibly a mechanism of embryonic arrest suppression by these genes that is not related to the cell cycle. This latter possibility is consistent with our previous findings that LIN-35 does not play a critical role in cell-cycle regulation in embryos (Kirienko and Fay 2007).

As a final test of the multi-phenotypic *lin-35* suppressors, we assayed suppression of a nonsynthetic *lin-35* phenotype. High-temperature arrest (HTA; 26°) has been reported for a number of class B synMuv genes, including *lin-35* (Petrella *et al.* 2011). Notably, RNAi of *mes-4* and *mrg-1* suppresses the *lin-35* HTA phenotype (Petrella *et al.* 2011). Testing of the 26 *lin-35*; *slr-2* RNAi suppressors confirmed suppression of *lin-35(n745)* by *mes-4* and *mrg-1* and also identified *hcf-1* as a strong suppressor of *lin-35* HTA (Figure S9). These results are consistent with HCF-1, MES-4, and MRG-1 playing a central role in opposing the activities of LIN-35.

Discussion

We have identified a new category of genes that we term the "multi-phenotypic *lin-35* suppressors" (MPLS). Our data indicate that these genes play opposing roles to the pocket protein ortholog *lin-35*/pRb in multiple developmental contexts (Figure 4). To our knowledge, this is the first genetic analysis in *C. elegans* that has sought to characterize the suppression of multiple, distinct synthetic phenotypes that have in common a single inactivated gene (in our case, *lin-35*). Our previous analyses of *lin-35*-synthetic mutants have suggested that unique sets of misregulated genes underlie the diversity of observed phenotypes (Fay *et al.* 2002, 2003, 2004; Bender *et al.* 2004, 2007; Cui *et al.* 2004; Kirienko *et al.* 2008). We propose that genes capable of suppressing multiple genetically related but phenotypically distinct synthetic phenotypes are likely to act at the level of the shared mutant gene or its core downstream targets. Differences in the spectrum of *lin-35*-synthetic phenotypes that are suppressed by individual MPLS genes may reflect tissue-specific differences in their expression patterns or requirements for activity (Figure 4). Alternatively, differences in the efficiency of RNAi within distinct tissues may account for the inability of certain MPLS genes to mediate suppression for some phenotypes. In general, the analysis of multi-phenotypic suppressors of synthetic interactions should lead to the identification of genes whose activities are most germane to the direct or central functions of the common mutated gene. This multi-stage screening strategy could be useful for the study of any broadly acting gene for which multiple phenotypically distinct synthetic phenotypes are available.

In addition to suppressing multiple *lin-35*-synthetic phenotypes, several of the identified suppressors (*e.g.*, *mes-4*) also suppress phenotypes associated with single mutants in a number of class B synMuv genes, including *lin-35*. *lin-35* is an established negative regulator of the RNAi response, and *lin-35* mutants are correspondingly hyper-sensitive to RNAi (Wang *et al.* 2005; Lehner *et al.* 2006; Ceron *et al.* 2007). Interestingly, several suppressors identified in our screen were previously shown to suppress *lin-35* hyper-sensitivity to RNAi, including *mes-4*, *sin-3*, M03C11.3, ZK1127.3, and *zfp-1* (Kim *et al.* 2005; Wang *et al.* 2005). *lin-35* mutants also exhibit a repetitive-transgene silencing phenotype that

is suppressed by *mes-4* and ZK1127.3 RNAi (Hsieh *et al.* 1999; Pirrotta 2002; Wang *et al.* 2005). Furthermore, *lin-35* mutants display ectopic expression of germline-specific genes in somatic tissues, a phenotype that is also suppressed by *mes-4* RNAi (Wang *et al.* 2005; Petrella *et al.* 2011). Misexpression of germline genes in the soma of synMuv B mutants has been proposed to account for the silencing of somatic transgenes in these mutants, as repetitive transgenes are typically silenced in the germline (Hsieh *et al.* 1999; Wang *et al.* 2005; Petrella *et al.* 2011; Praitis and Maduro 2011).

Most recently, a study by Petrella *et al.* (2011) revealed that *lin-35*, along with several other class B synMuv mutants, undergoes L1 larval arrest at 26°, a temperature at which wild-type worms are viable. Furthermore, HTA is likely due to the misexpression of one or more classes of genes within the intestine (Petrella *et al.* 2011). Interestingly, RNAi of *mes-4*, *mrg-1*, *hcf-1*, and *isw-1*, four genes that suppress multiple *lin-35*-synthetic phenotypes, strongly suppressed HTA (Figure S9) (Petrella *et al.* 2011). Notably, genes that were upregulated in *lin-35* single mutants at 26° returned to levels that were more similar to those of wild type in *lin-35*; *mes-4 (RNAi)* larvae, a corrective phenomenon not observed for genes that were downregulated in *lin-35* single mutants at 26°. Moreover, these mutual targets of LIN-35 and MES-4 included many intestine-associated genes along with germline genes. Given our findings that *lin-35*; *slr-2* mutants have defective intestines because of the misexpression of many intestinal genes and that *lin-35*; *slr-2* arrest is suppressed by *mes-4(RNAi)*, we can suggest that genes that are specifically upregulated in the intestines of *lin-35*; *slr-2* mutants lead to intestinal malfunction. This conclusion is supported by our observation that blunt inhibition of protein synthesis either by cycloheximide or G418 treatment (Figure 2) or by depletion of ribosome biogenesis genes (Figure 1) also leads to the suppression of *lin-35*; *slr-2* and *dpl-1*; *slr-2* larval arrest.

Work in multiple organisms has demonstrated that pRb complex members play a primarily repressive role in transcription, a function that is also conserved in *C. elegans* (Chi and Reinke 2006; Kirienko and Fay 2007). This is consistent with the majority of MPLS genes functioning in the opposite role—as transcriptional activators (Figure 4; Table 1). In fact, the broadest-acting *lin-35* suppressors encode orthologs of proteins present in several established transcriptional activating complexes. The evolutionarily conserved suppressors *hcf-1*, *set-2*, F52B11.1, and *mes-4* are orthologous to members of the Set1/COMPASS H3K4 methylation complex (Stec *et al.* 1998; Strahl *et al.* 2002; Wysocka *et al.* 2003; Yokoyama *et al.* 2004; Bender *et al.* 2006; Nimura *et al.* 2009; Mohan *et al.* 2011). SET-2 is an active H3K4 methyltransferase in *C. elegans* and F52B11.1 is a homolog of yeast Cps40, a factor that promotes H3K4 methylation, suggesting that a Set1/COMPASS-like complex is antagonistic to LIN-35 (Fisher *et al.* 2010; Xiao *et al.* 2011). Interestingly, although homologous to Set1, MES-4 is a well-characterized H3K36 methyltransferase in *C. elegans* and flies (Bell *et al.* 2007; Rechtsteiner *et al.* 2010; Xiao *et al.* 2011). Furthermore, MES-4 does not require colocalization with RNA polymerase II, a feature of its well-studied yeast homolog, Set2 (Furuhashi *et al.* 2010; Rechtsteiner *et al.* 2010). Currently, the role H3K36 methylation in regulating ongoing transcription, as well as the possible mechanism by which loss of this activity would suppress *lin-35*-synthetic phenotypes, remains unclear. The functions of *hcf-1* orthologs have been primarily studied in systems other than *C. elegans*. In HeLa cells, HCF1 physically interacts with multiple E2Fs and recruits the Set1 complex to E2F promoter regions (Tyagi *et al.* 2007). Furthermore, pRb complex members interact with the Set1/COMPASS methyltransferase complex in human cell culture to control the expression of cell-cycle genes (Reilly *et al.* 2002; Delehouzee *et al.* 2005). *mrg-1* and ZK1127.3 orthologs are members of multiple histone acetyltransferase complexes, including the NuA4 acetylation complex in budding yeast and the related Tip60 HAT complex in humans (Ceol and Horvitz 2004; Pena *et al.* 2011). Moreover, yeast two-hybrid analysis indicates that *mrg-1* and ZK1127.3 physically interact in *C. elegans*, whereas the human *mrg-1* ortholog MRG15 physically interacts with the ZK1127.3 ortholog MRGBP in HeLa cells (Cai *et al.* 2003; Li *et al.* 2004). Additionally, MRG15 physically interacts with pRb and has been proposed to play antagonistic roles in controlling E2F target regulation (Leung *et al.* 2001).

The above results suggest that both the Set1/COMPASS and NuA4/Tip60 complexes coregulate a set of conserved and overlapping targets with pRb and E2F family members. To examine this, we analyzed data from an HCF-1 ChIP-seq study carried out in mouse embryonic stem cells (Dejosez *et al.* 2010). Of the 305 HCF-1-bound genes identified, 151 had annotated orthologs in *C. elegans* and 23 of these were previously shown to be targets of LIN-35 by transcriptome analysis (Kirienko and Fay 2007). This represents an ~1.5 enrichment of HCF-1-bound genes among LIN-35 targets ($P = 0.05$, chi square test). Thus, LIN-35 and HCF-1 may possibly coregulate conserved targets across species. Moreover, greater overlap of LIN-35/pRb and HCF-1 targets might be expected in parallel ChiP-seq experiments carried out in the same species or cell type. Intriguingly, cell-cycle arrest in HCF-1 mutants in human tissue culture cells can be suppressed by loss of pRb activity, indicating that both the regulatory framework and the genetic suppressor relationship between these genes have been maintained (Reilly *et al.* 2002).

In addition to MPLS genes, other identified suppressors may enhance our understanding of the *lin-35*; *slr-2* arrest phenotype. For example, the ability of *lin-35*; *slr-2* mutants to reach adulthood following inhibition of the prohibitin genes *phb-1* and *phb-2* indicates that intestinal malfunction is not the direct cause of the observed L1 arrest. Rather, our findings suggest that *lin-35*; *slr-2* mutants arrest because of the activation of an L1 metabolic checkpoint, which can be overridden by increasing energy availability through the mobilization and utilization of fat stores. A similar effect was

also observed in *inx-6* mutants following inactivation of *phb-1* or *phb-2*, which are nutrient deprived because of impairment in food uptake (Figure 3). Thus, our studies have revealed a possible novel mechanism to suppress at least some aspects of nutrient deprivation-induced L1 diapause arrest.

In addition, it is perhaps surprising that gross inhibition of ribosome biogenesis and protein translation would prove to be an effective means to suppress a phenotype caused by the overexpression of a specific subset of proteins. Rather, if protein expression were to be uniformly reduced, imbalances in relative protein levels should persist. This might indicate that inhibition of protein synthesis in our suppressed strains is not uniform but may correlate with mRNA levels or translation rates, a phenomenon previously reported for cycloheximide-treated cells infected with virus (David 1976; Jen *et al.* 1978). We also note that inhibition of ribosome biogenesis was not effective at suppressing other *lin-35*-synthetic phenotypes. This finding may appear counterintuitive, given that suppression of most *lin-35*-associated phenotypes by SET1 and NuA4 complex members indicates that these phenotypes also result from the increased expression of LIN-35 targets. However, differences in the ability of the protein translation factors to suppress individual *lin-35*-synthetic phenotypes may depend more on specific changes in the secondary targets of LIN-35 and its synthetic lethal protein counterparts. For example, upregulated intestinal genes in *lin-35*; *slr-2* mutants are not thought to be direct targets of a LIN-35–EFL-1–DPL-1 complex (Kirienko *et al.* 2008). Thus, in the case of other *lin-35*-synthetic mutants, the proximal cause of the observed defects may not be due to the strongly elevated expression of multiple loci, and therefore these phenotypes may not be effectively alleviated by decreased protein synthesis. Nevertheless, our findings do suggest that phenotypes caused by multi-gene overexpression may be generally suppressible through the inhibition of protein synthesis.

Acknowledgments

We thank Amy Fluet, John Yochem, and Aleksandra Kuzmanov for critically reading the manuscript and Evguenia Karina, Olivia Wolpert, James Polek, and Aya Murakami for aid with RNAi screening. We also thank the *Caenorhabditis elegans* Genetics Center, the U.S./Canadian *C. elegans* knockout consortium, and the National Bioresource Project for the Experimental Animal *C. elegans* (Japan). This work was supported by grant GM066868 from the National Institutes of Health.

Literature Cited

Albanese, V., S. Reissmann, and J. Frydman, 2010 A ribosome-anchored chaperone network that facilitates eukaryotic ribosome biogenesis. J. Cell Biol. 189: 69–81.

Andersen, E. C., and H. R. Horvitz, 2007 Two C. elegans histone methyltransferases repress lin-3 EGF transcription to inhibit vulval development. Development 134: 2991–2999.

Andersen, E. C., X. Lu, and H. R. Horvitz, 2006 C. elegans ISWI and NURF301 antagonize an Rb-like pathway in the determination of multiple cell fates. Development 133: 2695–2704.

Artal-Sanz, M., and N. Tavernarakis, 2009a Prohibitin and mitochondrial biology. Trends Endocrinol. Metab. 20: 394–401.

Artal-Sanz, M., and N. Tavernarakis, 2009b Prohibitin couples diapause signalling to mitochondrial metabolism during ageing in C. elegans. Nature 461: 793–797.

Artal-Sanz, M., and N. Tavernarakis, 2010 Opposing function of mitochondrial prohibitin in aging. Aging (Albany NY) 2: 1004–1011.

Balciunaite, E., A. Spektor, N. H. Lents, H. Cam, H. Te Riele *et al.*, 2005 Pocket protein complexes are recruited to distinct targets in quiescent and proliferating cells. Mol. Cell. Biol. 25: 8166–8178.

Bassler, J., P. Grandi, O. Gadal, T. Lessmann, E. Petfalski *et al.*, 2001 Identification of a 60S preribosomal particle that is closely linked to nuclear export. Mol. Cell 8: 517–529.

Batsche, E., P. Moschopoulos, J. Desroches, S. Bilodeau, and J. Drouin, 2005 Retinoblastoma and the related pocket protein p107 act as coactivators of NeuroD1 to enhance gene transcription. J. Biol. Chem. 280: 16088–16095.

Beitel, G. J., E. J. Lambie, and H. R. Horvitz, 2000 The C. elegans gene lin-9,which acts in an Rb-related pathway, is required for gonadal sheath cell development and encodes a novel protein. Gene 254: 253–263.

Bell, O., C. Wirbelauer, M. Hild, A. N. Scharf, M. Schwaiger *et al.*, 2007 Localized H3K36 methylation states define histone H4K16 acetylation during transcriptional elongation in Drosophila. EMBO J. 26: 4974–4984.

Bender, A. M., O. Wells, and D. S. Fay, 2004 lin-35/Rb and xnp-1/ATR-X function redundantly to control somatic gonad development in C. elegans. Dev. Biol. 273: 335–349.

Bender, A. M., N. V. Kirienko, S. K. Olson, J. D. Esko, and D. S. Fay, 2007 lin-35/Rb and the CoREST ortholog spr-1 coordinately regulate vulval morphogenesis and gonad development in C. elegans. Dev. Biol. 302: 448–462.

Bender, L. B., J. Suh, C. R. Carroll, Y. Fong, I. M. Fingerman *et al.*, 2006 MES-4: an autosome-associated histone methyltransferase that participates in silencing the X chromosomes in the C. elegans germ line. Development 133: 3907–3917.

Bernstein, B. E., J. K. Tong, and S. L. Schreiber, 2000 Genome-wide studies of histone deacetylase function in yeast. Proc. Natl. Acad. Sci. USA 97: 13708–13713.

Black, E. P., E. Huang, H. Dressman, R. Rempel, N. Laakso *et al.*, 2003 Distinct gene expression phenotypes of cells lacking Rb and Rb family members. Cancer Res. 63: 3716–3723.

Bousquet-Antonelli, C., E. Vanrobays, J. P. Gelugne, M. Caizergues-Ferrer, and Y. Henry, 2000 Rrp8p is a yeast nucleolar protein functionally linked to Gar1p and involved in pre-rRNA cleavage at site A2. RNA 6: 826–843.

Cai, Y., J. Jin, C. Tomomori-Sato, S. Sato, I. Sorokina *et al.*, 2003 Identification of new subunits of the multiprotein mammalian TRRAP/TIP60-containing histone acetyltransferase complex. J. Biol. Chem. 278: 42733–42736.

Calo, E., J. A. Quintero-Estades, P. S. Danielian, S. Nedelcu, S. D. Berman *et al.*, 2010 Rb regulates fate choice and lineage commitment in vivo. Nature 466: 1110–1114.

Cao, L., B. Peng, L. Yao, X. Zhang, K. Sun *et al.*, 2010 The ancient function of RB-E2F pathway: insights from its evolutionary history. Biol. Direct 5: 55.

Ceol, C. J., and H. R. Horvitz, 2001 dpl-1 DP and efl-1 E2F act with lin-35 Rb to antagonize Ras signaling in C. elegans vulval development. Mol. Cell 7: 461–473.

Ceol, C. J., and H. R. Horvitz, 2004 A new class of C. elegans synMuv genes implicates a Tip60/NuA4-like HAT complex as a negative regulator of Ras signaling. Dev. Cell 6: 563–576.

Ceron, J., J. F. Rual, A. Chandra, D. Dupuy, M. Vidal *et al.*, 2007 Large-scale RNAi screens identify novel genes that interact

with the C. elegans retinoblastoma pathway as well as splicing-related components with synMuv B activity. BMC Dev. Biol. 7: 30.
Checchi, P. M., and W. G. Kelly, 2006 *emb-4* is a conserved gene required for efficient germline-specific chromatin remodeling during *Caenorhabditis elegans* embryogenesis. Genetics 174: 1895–1906.
Chen, D., R. Opavsky, M. Pacal, N. Tanimoto, P. Wenzel *et al.*, 2007 Rb-mediated neuronal differentiation through cell-cycle-independent regulation of E2f3a. PLoS Biol. 5: e179.
Chi, W., and V. Reinke, 2006 Promotion of oogenesis and embryogenesis in the C. elegans gonad by EFL-1/DPL-1 (E2F) does not require LIN-35 (pRB). Development 133: 3147–3157.
Chinnam, M., and D. W. Goodrich, 2011 RB1, development, and cancer. Curr. Top. Dev. Biol. 94: 129–169.
Cui, M., D. S. Fay, and M. Han, 2004 lin-35/Rb cooperates with the SWI/SNF complex to control *Caenorhabditis elegans* larval development. Genetics 167: 1177–1185.
Cui, M., E. B. Kim, and M. Han, 2006 Diverse chromatin remodeling genes antagonize the Rb-involved SynMuv pathways in C. elegans. PLoS Genet. 2: e74.
David, A. E., 1976 Control of vesicular stomatitis virus protein synthesis. Virology 71: 217–229.
De Falco, G., F. Comes, and C. Simone, 2006 pRb: master of differentiation. Coupling irreversible cell cycle withdrawal with induction of muscle-specific transcription. Oncogene 25: 5244–5249.
Dehe, P. M., and V. Geli, 2006 The multiple faces of Set1. Biochem. Cell Biol. 84: 536–548.
Dejosez, M., S. S. Levine, G. M. Frampton, W. A. Whyte, S. A. Stratton *et al.*, 2010 Ronin/Hcf-1 binds to a hyperconserved enhancer element and regulates genes involved in the growth of embryonic stem cells. Genes Dev. 24: 1479–1484.
de la Cruz, J., E. Sanz-Martinez, and M. Remacha, 2005 The essential WD-repeat protein Rsa4p is required for rRNA processing and intra-nuclear transport of 60S ribosomal subunits. Nucleic Acids Res. 33: 5728–5739.
Delehouzee, S., T. Yoshikawa, C. Sawa, J. Sawada, T. Ito *et al.*, 2005 GABP, HCF-1 and YY1 are involved in Rb gene expression during myogenesis. Genes Cells 10: 717–731.
Eisen, A., R. T. Utley, A. Nourani, S. Allard, P. Schmidt *et al.*, 2001 The yeast NuA4 and Drosophila MSL complexes contain homologous subunits important for transcription regulation. J. Biol. Chem. 276: 3484–3491.
Fay, D. S., and J. Yochem, 2007 The SynMuv genes of Caenorhabditis elegans in vulval development and beyond. Dev. Biol. 306: 1–9.
Fay, D. S., S. Keenan, and M. Han, 2002 fzr-1 and lin-35/Rb function redundantly to control cell proliferation in C. elegans as revealed by a nonbiased synthetic screen. Genes Dev. 16: 503–517.
Fay, D. S., E. Large, M. Han, and M. Darland, 2003 lin-35/Rb and ubc-18, an E2 ubiquitin-conjugating enzyme, function redundantly to control pharyngeal morphogenesis in C. elegans. Development 130: 3319–3330.
Fay, D. S., X. Qiu, E. Large, C. P. Smith, S. Mango *et al.*, 2004 The coordinate regulation of pharyngeal development in C. elegans by lin-35/Rb, pha-1, and ubc-18. Dev. Biol. 271: 11–25.
Ferguson, E. L., and H. R. Horvitz, 1989 The multivulva phenotype of certain *Caenorhabditis elegans* mutants results from defects in two functionally redundant pathways. Genetics 123: 109–121.
Fisher, K., S. M. Southall, J. R. Wilson, and G. B. Poulin, 2010 Methylation and demethylation activities of a C. elegans MLL-like complex attenuate RAS signalling. Dev. Biol. 341: 142–153.
Fukushige, T., M. G. Hawkins, and J. D. McGhee, 1998 The GATA-factor elt-2 is essential for formation of the Caenorhabditis elegans intestine. Dev. Biol. 198: 286–302.
Fukuyama, M., A. E. Rougvie, and J. H. Rothman, 2006 C. elegans DAF-18/PTEN mediates nutrient-dependent arrest of cell cycle and growth in the germline. Curr. Biol. 16: 773–779.
Furuhashi, H., T. Takasaki, A. Rechtsteiner, T. Li, H. Kimura *et al.*, 2010 Trans-generational epigenetic regulation of C. elegans primordial germ cells. Epigenetics Chromatin 3: 15.
Fusaro, G., S. Wang, and S. Chellappan, 2002 Differential regulation of Rb family proteins and prohibitin during camptothecin-induced apoptosis. Oncogene 21: 4539–4548.
Galani, K., T. A. Nissan, E. Petfalski, D. Tollervey, and E. Hurt, 2004 Rea1, a dynein-related nuclear AAA-ATPase, is involved in late rRNA processing and nuclear export of 60 S subunits. J. Biol. Chem. 279: 55411–55418.
Gery, S., A. F. Gombart, Y. K. Fung, and H. P. Koeffler, 2004 C/EBPepsilon interacts with retinoblastoma and E2F1 during granulopoiesis. Blood 103: 828–835.
Gu, T., S. Orita, and M. Han, 1998 Caenorhabditis elegans SUR-5, a novel but conserved protein, negatively regulates LET-60 Ras activity during vulval induction. Mol. Cell. Biol. 18: 4556–4564.
Halbach, A., H. Zhang, A. Wengi, Z. Jablonska, I. M. Gruber *et al.*, 2009 Cotranslational assembly of the yeast SET1C histone methyltransferase complex. EMBO J. 28: 2959–2970.
Hanazawa, M., I. Kawasaki, H. Kunitomo, K. Gengyo-Ando, K. L. Bennett *et al.*, 2004 The Caenorhabditis elegans eukaryotic initiation factor 5A homologue, IFF-1, is required for germ cell proliferation, gametogenesis and localization of the P-granule component PGL-1. Mech. Dev. 121: 213–224.
Hang, M., and M. M. Smith, 2011 Genetic analysis implicates the Set3/Hos2 histone deacetylase in the deposition and remodeling of nucleosomes containing H2A.Z. Genetics 187: 1053–1066.
Harrison, M. M., C. J. Ceol, X. Lu, and H. R. Horvitz, 2006 Some C. elegans class B synthetic multivulva proteins encode a conserved LIN-35 Rb-containing complex distinct from a NuRD-like complex. Proc. Natl. Acad. Sci. USA 103: 16782–16787.
Hsieh, J., J. Liu, S. A. Kostas, C. Chang, P. W. Sternberg *et al.*, 1999 The RING finger/B-box factor TAM-1 and a retinoblastoma-like protein LIN-35 modulate context-dependent gene silencing in Caenorhabditis elegans. Genes Dev. 13: 2958–2970.
Hua, H., and N. Sarvetnick, 2007 Expression of Id1 in adult, regenerating and developing pancreas. Endocrine 32: 280–286.
Jen, G., C. H. Birge, and R. E. Thach, 1978 Comparison of initiation rates of encephalomyocarditis virus and host protein synthesis in infected cells. J. Virol. 27: 640–647.
Ji, Y., and G. P. Studzinski, 2004 Retinoblastoma protein and CCAAT/enhancer-binding protein beta are required for 1,25-dihydroxyvitamin D3-induced monocytic differentiation of HL60 cells. Cancer Res. 64: 370–377.
Kamath, R. S., A. G. Fraser, Y. Dong, G. Poulin, R. Durbin *et al.*, 2003 Systematic functional analysis of the Caenorhabditis elegans genome using RNAi. Nature 421: 231–237.
Killian, D. J., and E. J. Hubbard, 2004 C. elegans pro-1 activity is required for soma/germline interactions that influence proliferation and differentiation in the germ line. Development 131: 1267–1278.
Kim, J. K., H. W. Gabel, R. S. Kamath, M. Tewari, A. Pasquinelli *et al.*, 2005 Functional genomic analysis of RNA interference in C. elegans. Science 308: 1164–1167.
Kim, Y. C., S. Y. Kim, J. M. Mellado-Gil, H. Yadav, W. Neidermyer *et al.*, 2011 RB regulates pancreas development by stabilizing Pdx1. EMBO J. 30: 1563–1576.
Kirienko, N. V., and D. S. Fay, 2007 Transcriptome profiling of the C. elegans Rb ortholog reveals diverse developmental roles. Dev. Biol. 305: 674–684.
Kirienko, N. V., J. D. McEnerney, and D. S. Fay, 2008 Coordinated regulation of intestinal functions in C. elegans by LIN-35/Rb and SLR-2. PLoS Genet. 4: e1000059.
Kirienko, N. V., K. Mani, and D. S. Fay, 2010 Cancer models in Caenorhabditis elegans. Dev. Dyn. 239: 1413–1448.
Kleivi, K., G. E. Lind, C. B. Diep, G. I. Meling, L. T. Brandal *et al.*, 2007 Gene expression profiles of primary colorectal carcinomas, liver metastases, and carcinomatoses. Mol. Cancer 6: 2.

Knudsen, E. S., and K. E. Knudsen, 2006 Retinoblastoma tumor suppressor: where cancer meets the cell cycle. Exp. Biol. Med. (Maywood) 231: 1271–1281.
Knudson, A. G. Jr.. 1971 Mutation and cancer: statistical study of retinoblastoma. Proc. Natl. Acad. Sci. USA 68: 820–823.
Komatsu, H., M. Y. Chao, J. Larkins-Ford, M. E. Corkins, G. A. Somers *et al.*, 2008 OSM-11 facilitates LIN-12 Notch signaling during Caenorhabditis elegans vulval development. PLoS Biol. 6: e196.
Krogan, N. J., W. T. Peng, G. Cagney, M. D. Robinson, R. Haw *et al.*, 2004 High-definition macromolecular composition of yeast RNA-processing complexes. Mol. Cell 13: 225–239.
Lasorella, A., M. Noseda, M. Beyna, Y. Yokota, and A. Iavarone, 2000 Id2 is a retinoblastoma protein target and mediates signalling by Myc oncoproteins. Nature 407: 592–598.
Lasorella, A., G. Rothschild, Y. Yokota, R. G. Russell, and A. Iavarone, 2005 Id2 mediates tumor initiation, proliferation, and angiogenesis in Rb mutant mice. Mol. Cell. Biol. 25: 3563–3574.
Lehner, B., A. Calixto, C. Crombie, J. Tischler, A. Fortunato *et al.*, 2006 Loss of LIN-35, the Caenorhabditis elegans ortholog of the tumor suppressor p105Rb, results in enhanced RNA interference. Genome Biol. 7: R4.
Leung, J. K., N. Berube, S. Venable, S. Ahmed, N. Timchenko *et al.*, 2001 MRG15 activates the B-myb promoter through formation of a nuclear complex with the retinoblastoma protein and the novel protein PAM14. J. Biol. Chem. 276: 39171–39178.
Li, S., J. A. Dent, and R. Roy, 2003 Regulation of intermuscular electrical coupling by the Caenorhabditis elegans innexin inx-6. Mol. Biol. Cell 14: 2630–2644.
Li, S., C. M. Armstrong, N. Bertin, H. Ge, S. Milstein *et al.*, 2004 A map of the interactome network of the metazoan C. elegans. Science 303: 540–543.
Li, T., and W. G. Kelly, 2011 A role for Set1/MLL-related components in epigenetic regulation of the Caenorhabditis elegans germ line. PLoS Genet. 7: e1001349.
Lo, K. Y., Z. Li, C. Bussiere, S. Bresson, E. M. Marcotte *et al.*, 2010 Defining the pathway of cytoplasmic maturation of the 60S ribosomal subunit. Mol. Cell 39: 196–208.
Lu, X., and H. R. Horvitz, 1998 lin-35 and lin-53, two genes that antagonize a C. elegans Ras pathway, encode proteins similar to Rb and its binding protein RbAp48. Cell 95: 981–991.
Mani, K., and D. S. Fay, 2009 A mechanistic basis for the coordinated regulation of pharyngeal morphogenesis in Caenorhabditis elegans by LIN-35/Rb and UBC-18-ARI-1. PLoS Genet. 5: e1000510.
Markey, M. P., S. P. Angus, M. W. Strobeck, S. L. Williams, R. W. Gunawardena *et al.*, 2002 Unbiased analysis of RB-mediated transcriptional repression identifies novel targets and distinctions from E2F action. Cancer Res. 62: 6587–6597.
Mello, C. C., J. M. Kramer, D. Stinchcomb, and V. Ambros, 1991 Efficient gene transfer in C.elegans: extrachromosomal maintenance and integration of transforming sequences. EMBO J. 10: 3959–3970.
Milkereit, P., O. Gadal, A. Podtelejnikov, S. Trumtel, N. Gas *et al.*, 2001 Maturation and intranuclear transport of pre-ribosomes requires Noc proteins. Cell 105: 499–509.
Mishra, S., L. C. Murphy, and L. J. Murphy, 2006 The prohibitins: emerging roles in diverse functions. J. Cell. Mol. Med. 10: 353–363.
Mishra, S., S. R. Ande, and B. L. Nyomba, 2010 The role of prohibitin in cell signaling. FEBS J. 277: 3937–3946.
Mohan, M., H. M. Herz, E. R. Smith, Y. Zhang, J. Jackson *et al.*, 2011 The COMPASS family of H3K4 methylases in Drosophila. Mol. Cell. Biol. 31: 4310–4318.
Morris, E. J., and N. J. Dyson, 2001 Retinoblastoma protein partners. Adv. Cancer Res. 82: 1–54.
Muller, H., A. P. Bracken, R. Vernell, M. C. Moroni, F. Christians *et al.*, 2001 E2Fs regulate the expression of genes involved in differentiation, development, proliferation, and apoptosis. Genes Dev. 15: 267–285.
Murton, B. L., W. L. Chin, C. P. Ponting, and L. S. Itzhaki, 2010 Characterising the binding specificities of the subunits associated with the KMT2/Set1 histone lysine methyltransferase. J. Mol. Biol. 398: 481–488.
Nimura, K., K. Ura, H. Shiratori, M. Ikawa, M. Okabe *et al.*, 2009 A histone H3 lysine 36 trimethyltransferase links Nkx2–5 to Wolf-Hirschhorn syndrome. Nature 460: 287–291.
O'Rourke, E. J., A. A. Soukas, C. E. Carr, and G. Ruvkun, 2009 C. elegans major fats are stored in vesicles distinct from lysosome-related organelles. Cell Metab. 10: 430–435.
Osman, C., C. Merkwirth, and T. Langer, 2009 Prohibitins and the functional compartmentalization of mitochondrial membranes. J. Cell Sci. 122: 3823–3830.
Page, B. D., S. Guedes, D. Waring, and J. R. Priess, 2001 The C. elegans E2F- and DP-related proteins are required for embryonic asymmetry and negatively regulate Ras/MAPK signaling. Mol. Cell 7: 451–460.
Paternot, S., L. Bockstaele, X. Bisteau, H. Kooken, K. Coulonval *et al.*, 2010 Rb inactivation in cell cycle and cancer: the puzzle of highly regulated activating phosphorylation of CDK4 *vs.* constitutively active CDK-activating kinase. Cell Cycle 9: 689–699.
Pena, A. N., K. Tominaga, and O. M. Pereira-Smith, 2011 MRG15 activates the cdc2 promoter via histone acetylation in human cells. Exp. Cell Res. 317: 1534–1540.
Petrella, L. N., W. Wang, C. A. Spike, A. Rechtsteiner, V. Reinke *et al.*, 2011 synMuv B proteins antagonize germline fate in the intestine and ensure C. elegans survival. Development 138: 1069–1079.
Pirrotta, V., 2002 Silence in the germ. Cell 110: 661–664.
Poznic, M., 2009 Retinoblastoma protein: a central processing unit. J. Biosci. 34: 305–312.
Praitis, V., and M. F. Maduro, 2011 Transgenesis in C. elegans. Methods Cell Biol. 106: 161–185.
Qiu, X., and D. S. Fay, 2006 ARI-1, an RBR family ubiquitin-ligase, functions with UBC-18 to regulate pharyngeal development in C. elegans. Dev. Biol. 291: 239–252.
Rechtsteiner, A., S. Ercan, T. Takasaki, T. M. Phippen, T. A. Egelhofer *et al.*, 2010 The histone H3K36 methyltransferase MES-4 acts epigenetically to transmit the memory of germline gene expression to progeny. PLoS Genet. 6**:** pii: e1001091.
Reilly, P. T., J. Wysocka, and W. Herr, 2002 Inactivation of the retinoblastoma protein family can bypass the HCF-1 defect in tsBN67 cell proliferation and cytokinesis. Mol. Cell. Biol. 22: 6767–6778.
Rekhtman, N., K. S. Choe, I. Matushansky, S. Murray, T. Stopka *et al.*, 2003 PU.1 and pRB interact and cooperate to repress GATA-1 and block erythroid differentiation. Mol. Cell. Biol. 23: 7460–7474.
Rodenas, E., E. P. Klerkx, C. Ayuso, A. Audhya, and P. Askjaer, 2009 Early embryonic requirement for nucleoporin Nup35/NPP-19 in nuclear assembly. Dev. Biol. 327: 399–409.
Rual, J. F., J. Ceron, J. Koreth, T. Hao, A. S. Nicot *et al.*, 2004 Toward improving Caenorhabditis elegans phenome mapping with an ORFeome-based RNAi library. Genome Res. 14: 2162–2168.
Sabelli, P. A., and B. A. Larkins, 2006 Grasses like mammals? Redundancy and compensatory regulation within the retinoblastoma protein family. Cell Cycle 5: 352–355.
Schreiber, M. A., J. T. Pierce-Shimomura, S. Chan, D. Parry, and S. L. McIntire, 2010 Manipulation of behavioral decline in Caenorhabditis elegans with the Rag GTPase raga-1. PLoS Genet. 6: e1000972.
Sherr, C. J., 1996 Cancer cell cycles. Science 274: 1672–1677.
Sherr, C. J., and F. McCormick, 2002 The RB and p53 pathways in cancer. Cancer Cell 2: 103–112.
Shi, X., I. Kachirskaia, K. L. Walter, J. H. Kuo, A. Lake *et al.*, 2007 Proteome-wide analysis in Saccharomyces cerevisiae identifies several PHD fingers as novel direct and selective binding modules of histone H3 methylated at either lysine 4 or lysine 36. J. Biol. Chem. 282: 2450–2455.

Silverstein, R. A., and K. Ekwall, 2005 Sin3: a flexible regulator of global gene expression and genome stability. Curr. Genet. 47: 1–17.
Simonet, T., R. Dulermo, S. Schott, and F. Palladino, 2007 Antagonistic functions of SET-2/SET1 and HPL/HP1 proteins in C. elegans development. Dev. Biol. 312: 367–383.
Soukas, A. A., E. A. Kane, C. E. Carr, J. A. Melo, and G. Ruvkun, 2009 Rictor/TORC2 regulates fat metabolism, feeding, growth, and life span in Caenorhabditis elegans. Genes Dev. 23: 496–511.
Stec, I., T. J. Wright, G. J. van Ommen, P. A. de Boer, A. van Haeringen *et al.*, 1998 WHSC1, a 90 kb SET domain-containing gene, expressed in early development and homologous to a Drosophila dysmorphy gene maps in the Wolf-Hirschhorn syndrome critical region and is fused to IgH in t(4;14) multiple myeloma. Hum. Mol. Genet. 7: 1071–1082.
Stiernagle, T. 2006 Maintenance of *C. elegans* (February 11, 2006), *WormBook*, ed. The *C. elegans* Research Community, WormBook, doi/10.1895/wormbook.1.101.1, http://www.wormbook.org.
Strahl, B. D., P. A. Grant, S. D. Briggs, Z. W. Sun, J. R. Bone *et al.*, 2002 Set2 is a nucleosomal histone H3-selective methyltransferase that mediates transcriptional repression. Mol. Cell. Biol. 22: 1298–1306.
Sulston, J. E., and H. R. Horvitz, 1977 Post-embryonic cell lineages of the nematode, Caenorhabditis elegans. Dev. Biol. 56: 110–156.
Takahashi, C., B. Contreras, R. T. Bronson, M. Loda, and M. E. Ewen, 2004 Genetic interaction between Rb and K-ras in the control of differentiation and tumor suppression. Mol. Cell. Biol. 24: 10406–10415.
Takasaki, T., Z. Liu, Y. Habara, K. Nishiwaki, J. Nakayama *et al.*, 2007 MRG-1, an autosome-associated protein, silences X-linked genes and protects germline immortality in Caenorhabditis elegans. Development 134: 757–767.
Thomas, D. M., S. A. Carty, D. M. Piscopo, J. S. Lee, W. F. Wang *et al.*, 2001 The retinoblastoma protein acts as a transcriptional coactivator required for osteogenic differentiation. Mol. Cell 8: 303–316.
Thomas, J. H., and H. R. Horvitz, 1999 The C. elegans gene lin-36 acts cell autonomously in the lin-35 Rb pathway. Development 126: 3449–3459.
Thomas, J. H., C. J. Ceol, H. T. Schwartz, and H. R. Horvitz, 2003 New genes that interact with lin-35 Rb to negatively regulate the let-60 ras pathway in *Caenorhabditis elegans*. Genetics 164: 135–151.
Timmons, L., 2006 Delivery methods for RNA interference in C. elegans. Methods Mol. Biol. 351: 119–125.
Timmons, L., D. L. Court, and A. Fire, 2001 Ingestion of bacterially expressed dsRNAs can produce specific and potent genetic interference in Caenorhabditis elegans. Gene 263: 103–112.
Tyagi, S., A. L. Chabes, J. Wysocka, and W. Herr, 2007 E2F activation of S phase promoters via association with HCF-1 and the MLL family of histone H3K4 methyltransferases. Mol. Cell 27: 107–119.
Van Aken, O., J. Whelan, and F. Van Breusegem, 2010 Prohibitins: mitochondrial partners in development and stress response. Trends Plant Sci. 15: 275–282.
van den Heuvel, S., and N. J. Dyson, 2008 Conserved functions of the pRB and E2F families. Nat. Rev. Mol. Cell Biol. 9: 713–724.
Vanrobays, E., P. E. Gleizes, C. Bousquet-Antonelli, J. Noaillac-Depeyre, M. Caizergues-Ferrer *et al.*, 2001 Processing of 20S pre-rRNA to 18S ribosomal RNA in yeast requires Rrp10p, an essential non-ribosomal cytoplasmic protein. EMBO J. 20: 4204–4213.
Viatour, P., and J. Sage, 2011 Newly identified aspects of tumor suppression by RB. Dis. Model Mech. 4: 581–585.
Voutev, R., D. J. Killian, J. H. Ahn, and E. J. Hubbard, 2006 Alterations in ribosome biogenesis cause specific defects in C. elegans hermaphrodite gonadogenesis. Dev. Biol. 298: 45–58.
Walkley, C. R., V. G. Sankaran, and S. H. Orkin, 2008 Rb and hematopoiesis: stem cells to anemia. Cell Div. 3: 13.
Wang, D., S. Kennedy, D. Conte Jr., J. K. Kim, H. W. Gabel *et al.*, 2005 Somatic misexpression of germline P granules and enhanced RNA interference in retinoblastoma pathway mutants. Nature 436: 593–597.
Wang, S., N. Nath, M. Adlam, and S. Chellappan, 1999a Prohibitin, a potential tumor suppressor, interacts with RB and regulates E2F function. Oncogene 18: 3501–3510.
Wang, S., N. Nath, G. Fusaro, and S. Chellappan, 1999b Rb and prohibitin target distinct regions of E2F1 for repression and respond to different upstream signals. Mol. Cell. Biol. 19: 7447–7460.
Wang, S., G. Fusaro, J. Padmanabhan, and S. P. Chellappan, 2002 Prohibitin co-localizes with Rb in the nucleus and recruits N-CoR and HDAC1 for transcriptional repression. Oncogene 21: 8388–8396.
Wheeler, J. M., and J. H. Thomas, 2006 Identification of a novel gene family involved in osmotic stress response in *Caenorhabditis elegans*. Genetics 174: 1327–1336.
Wikenheiser-Brokamp, K. A., 2006 Retinoblastoma family proteins: insights gained through genetic manipulation of mice. Cell. Mol. Life Sci. 63: 767–780.
Witkiewicz, A. K., K. E. Knudsen, A. P. Dicker, and E. S. Knudsen, 2011 The meaning of p16(ink4a) expression in tumors: functional significance, clinical associations and future developments. Cell Cycle 10: 2497–2503.
Wu, M., P. F. Wang, J. S. Lee, S. Martin-Brown, L. Florens *et al.*, 2008 Molecular regulation of H3K4 trimethylation by Wdr82, a component of human Set1/COMPASS. Mol. Cell. Biol. 28: 7337–7344.
Wysocka, J., M. P. Myers, C. D. Laherty, R. N. Eisenman, and W. Herr, 2003 Human Sin3 deacetylase and trithorax-related Set1/Ash2 histone H3–K4 methyltransferase are tethered together selectively by the cell-proliferation factor HCF-1. Genes Dev. 17: 896–911.
Xiao, Y., C. Bedet, V. J. Robert, T. Simonet, S. Dunkelbarger *et al.*, 2011 Caenorhabditis elegans chromatin-associated proteins SET-2 and ASH-2 are differentially required for histone H3 Lys 4 methylation in embryos and adult germ cells. Proc. Natl. Acad. Sci. USA 108: 8305–8310.
Xie, Y., and A. Varshavsky, 2000 Physical association of ubiquitin ligases and the 26S proteasome. Proc. Natl. Acad. Sci. USA 97: 2497–2502.
Xu, L., and S. Strome, 2001 Depletion of a novel SET-domain protein enhances the sterility of *mes-3* and *mes-4* mutants of *Caenorhabditis elegans*. Genetics 159: 1019–1029.
Yokoyama, A., Z. Wang, J. Wysocka, M. Sanyal, D. J. Aufiero *et al.*, 2004 Leukemia proto-oncoprotein MLL forms a SET1-like histone methyltransferase complex with menin to regulate Hox gene expression. Mol. Cell. Biol. 24: 5639–5649.
Zanelli, C. F., and S. R. Valentini, 2007 Is there a role for eIF5A in translation? Amino Acids 33: 351–358.
Zaros, C., and P. Thuriaux, 2005 Rpc25, a conserved RNA polymerase III subunit, is critical for transcription initiation. Mol. Microbiol. 55: 104–114.

Communicating editor: P. Sengupta

GENETICS

Supporting Information
http://www.genetics.org/content/suppl/2012/04/27/genetics.112.140152.DC1

A Network of Genes Antagonistic to the LIN-35 Retinoblastoma Protein of *Caenorhabditis elegans*

Stanley R. G. Polley and David S. Fay

Copyright © 2012 by the Genetics Society of America
DOI: 10.1534/genetics.112.140152

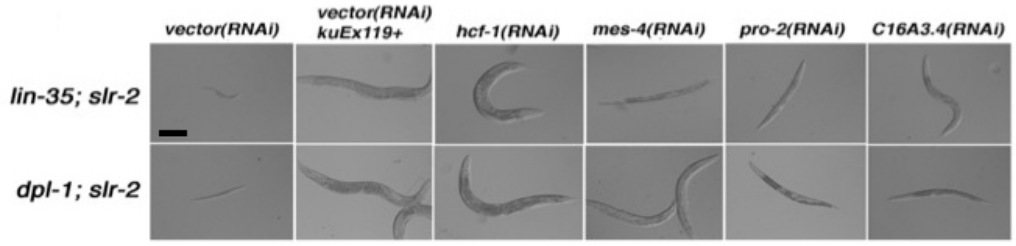

Figure S1 Representative DIC images of suppressed animals for both *lin-35; slr-2* and *dpl-1; slr-2* with the indicated RNAi. Control vector*(RNAi)* shows the typical L1 arrest of *lin-35; slr-2* or *dpl-2; slr-2* double mutants. *kuEx119* is an extrachromosomal array that contains wild-type rescuing sequences for *lin-35*, thereby allowing double mutants to reach the adult stage. Note that RNAi treatments for *mes-4*, *pro-2*, and *C16A3.4* lead to bypass of L1 arrest but do not generally result in full-size fertile adults. Size bar is 100 μm for all panels.

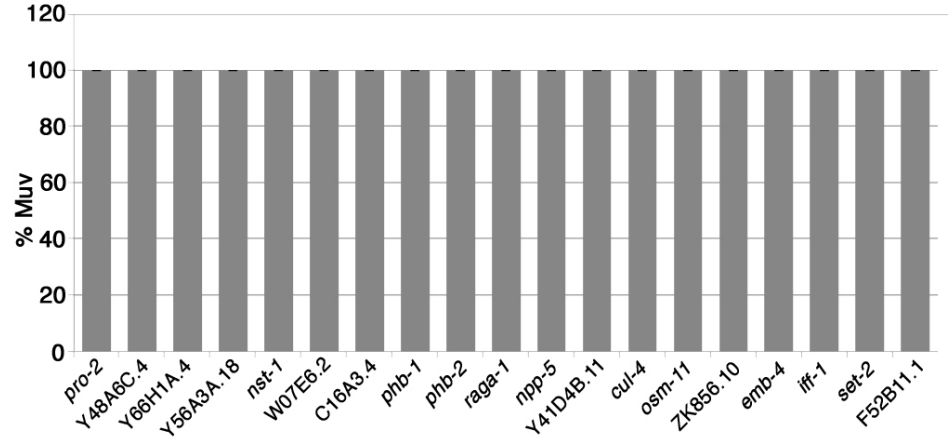

Figure S2 Lack of suppression of *lin-15ab* synMuv by novel *lin-35; slr-2* suppressors. Percent suppression of Muv by the 18 *lin-35; slr-2* suppressors not previously identified as SynMuv suppressors. Error bars represent 95% confidence intervals.

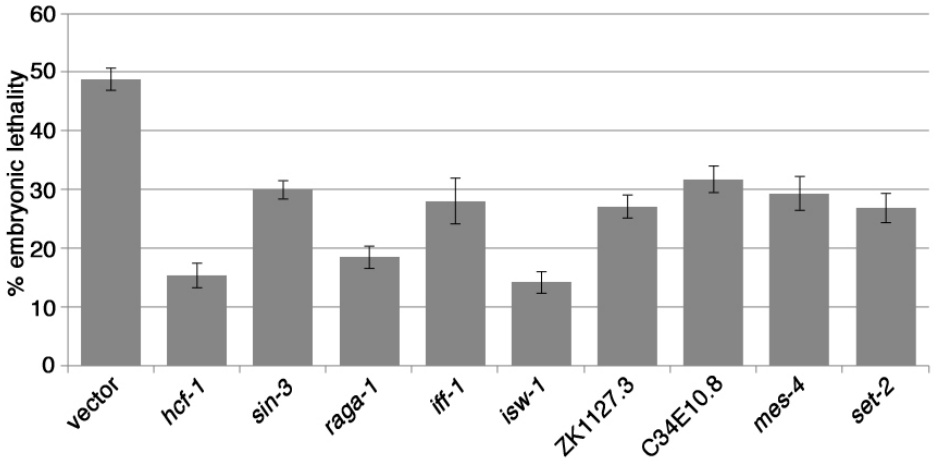

Figure S3 RNAi suppressors of *lin-35; fzr-1* embryonic arrest. Percent suppression of *lin-35; fzr-1* embryonic lethality (emb). All 26 sequence-confirmed RNAi clones isolated from the *lin-35; slr-2* screen and all previously characterized synMuv suppressors were tested. Only positive clones are shown ($P < 0.05$). Vector denotes a control RNAi. Error bars represent 95% confidence intervals.

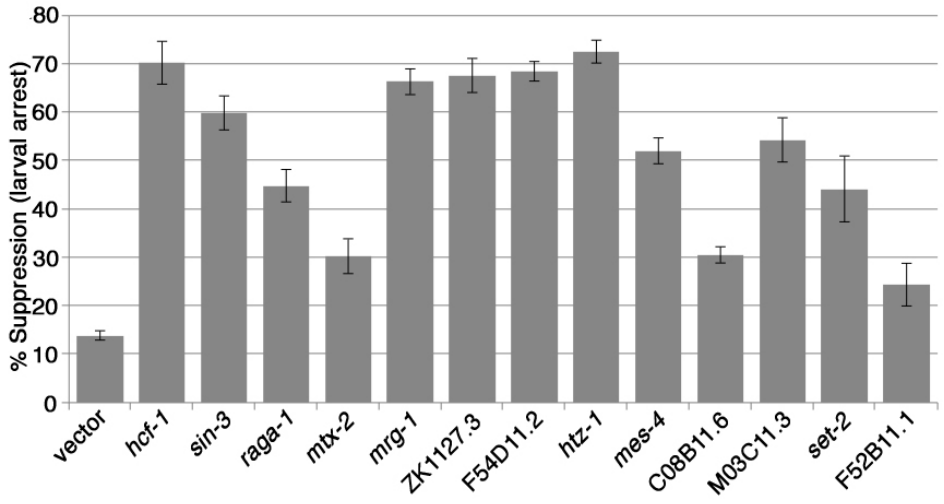

Figure S4 RNAi suppressors of *lin-35; spr-1.* Percent suppression of *lin-35; spr-1* larval arrest. All 26 sequence-confirmed RNAi clones isolated from the *lin-35; slr-2* screen and all previously characterized synMuv suppressors were tested. Only positive clones are shown ($P < 0.05$). Vector denotes a control RNAi. Error bars represent 95% confidence intervals.

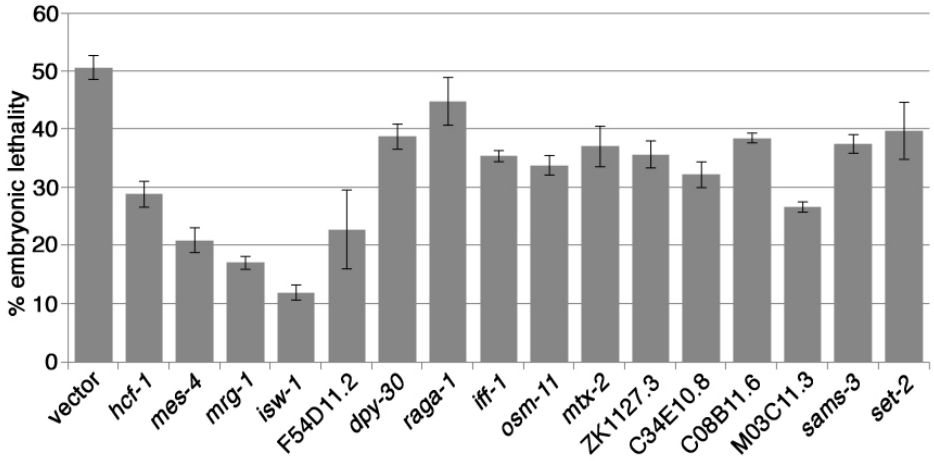

Figure S5 RNAi suppressors of *lin-35 xnp-1.* Percent suppression of *lin-35 xnp-1* embryonic lethality. All 26 sequence-confirmed RNAi clones isolated from the *lin-35; slr-2* screen and all previously characterized synMuv suppressors were tested. Only positive clones are shown ($P < 0.05$). Vector denotes a control RNAi. Error bars represent 95% confidence intervals.

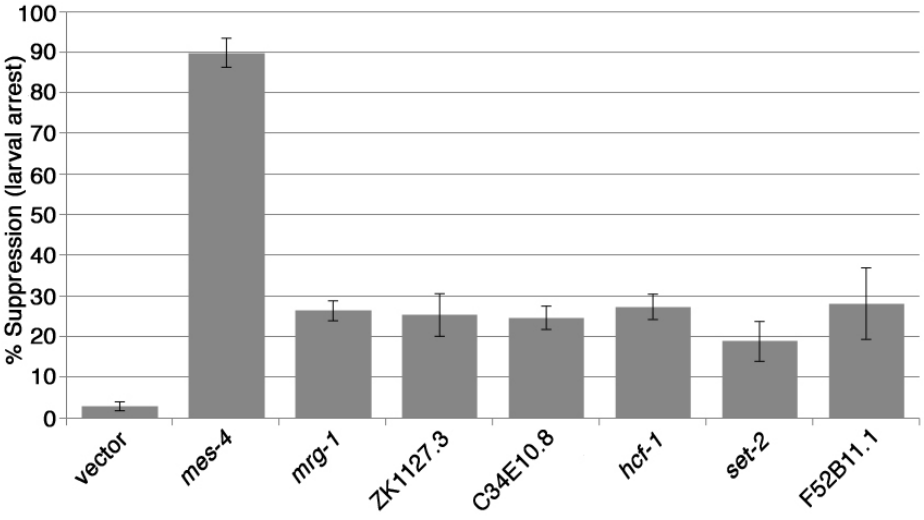

Figure S6 RNAi suppressors of *lin-35 psa-1.* Percent suppression of *lin-35; psa-1* larval arrest. All 26 sequence-confirmed RNAi clones isolated from the *lin-35; slr-2* screen and all previously characterized synMuv suppressors were tested. Only positive clones are shown ($P < 0.05$). Vector denotes a control RNAi. Error bars represent 95% confidence intervals.

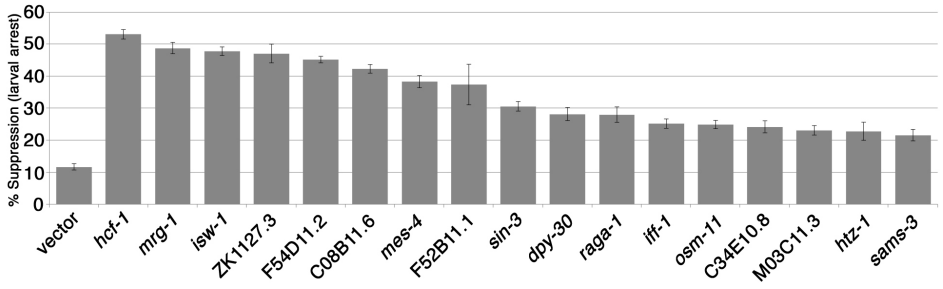

Figure S7 RNAi suppressors of *lin-35; ubc-18.* Percent suppression of *lin-35; ubc-18* larval arrest. All 26 sequence-confirmed RNAi clones isolated from the *lin-35; slr-2* screen and all previously characterized synMuv suppressors were tested. Only positive clones are shown ($P < 0.05$). Vector denotes a control RNAi. Error bars represent 95% confidence intervals.

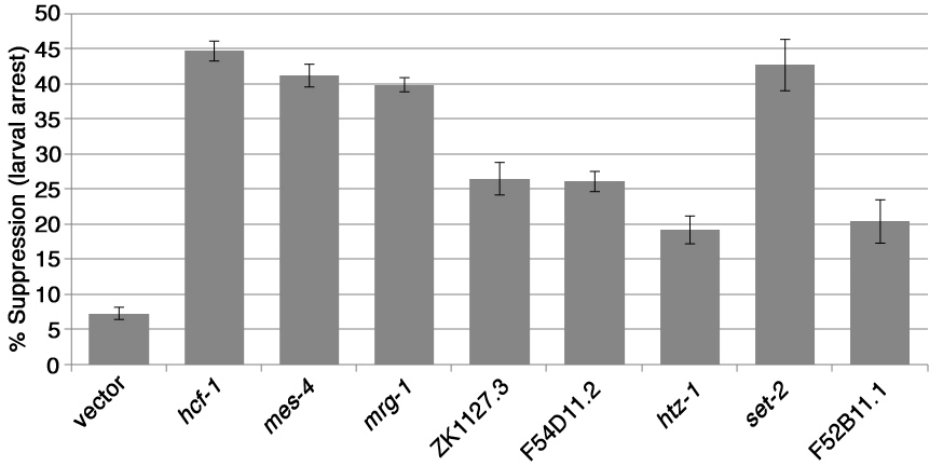

Figure S8 RNAi suppressors of *lin-35; pha-1.* Percent suppression of *lin-35; pha-1* larval arrest. All 26 sequence-confirmed RNAi clones isolated from the *lin-35; slr-2* screen and all previously characterized synMuv suppressors were tested. Only positive clones are shown ($P < 0.05$). Vector denotes a control RNAi. Error bars represent 95% confidence intervals.

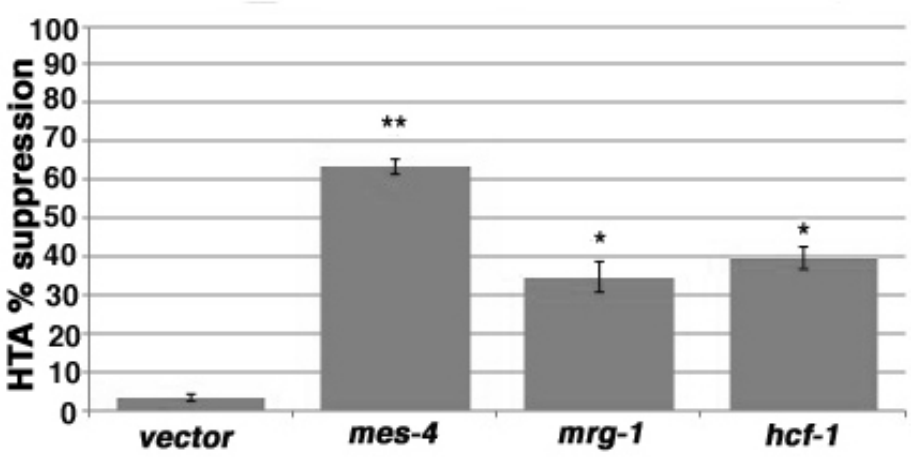

Figure S9 RNAi suppression of *lin-35* HTA. Percentage of *lin-35(745)* mutants incubated at 26° on RNAi plates that develop beyond the L1 larval stage. All 26 sequence-confirmed RNAi clones isolated from the *lin-35; slr-2* screen and all previously characterized synMuv suppressors were tested. Only positive clones are shown: *, $P < 0.05$; **, $P < 0.01$. Error bars represent 95% confidence intervals.

Table S1 lin-35; slr-2 suppressor phenotypes

Genes sorted by category	*% lin-35; slr-2* Suppression[a]	Terminal Stage Reached	Reported RNAi phenotype[b]
Ribosome Biogenesis			
pro-2	19.4	Sterile adult	larval arrest, emb, gro,
nst-1	27.8	Sterile adult	larval arrest, gro
Y48A6C.4	45.1	Sterile adult	larval arrest, gro
Y56A3A.18	30.6	Sterile adult	emb, gro, ste
Y66H1A.4	35.2	Sterile adult	gro, ste
W07E6.2	42.7	Sterile adult	larval arrest, gro, ste
C16A3.4	66.1	Sterile adult	emb, gro, ste
Mitochondrial Prohibitins			
phb-1	41.9	Sterile adult	emb
phb-2	32.2	Sterile adult	emb, gro, ste
SynMuv Suppressors			
hcf-1	48.6	Fertile adult	No growth phenotypes[c]
mes-4	18.8	Fertile adult	emb, ste
mrg-1	27.9	Fertile adult	larval arrest, ste
wdr-5.1	20.7	Sterile adult	ste
hecd-1	20.0	Fertile adult	let
dpy-30	19.9	Sterile adult	emb, gro, let
sin-3	15.9	Fertile adult	No growth phenotype
zfp-1	7.7	Sterile adult	emb, gro, ste
Other			
raga-1	10.2	Fertile adult	larval arrest , emb, gro
npp-5	7.9	L2/L3	emb, gro
Y41D4B.11	15.8	Sterile adult	gro, ste
cul-4	7.8	L2/L3	gro, ste
osm-11	10.9	Sterile adult	No growth phenotypes[c]
ZK856.10	8.3	Sterile adult	larval arrest, gro, ste
emb-4	6.8	L2/L3	emb, gro
iff-1	9.8	Sterile adult	emb, ste
mtx-2	7.9	Sterile adult	None reported

[a] Corresponds to Figure 1.
[b] Based on WormBase annotation of RNAi phenotypes. Includes both N2 and RNAi-hypersensitive backgrounds.
[c] No reported phenotypes effecting growth or fertility. May have other reported phenotypes.

Table S2 synMuv suppressors tested for suppression of *lin-35*-synthetic phenotypes

Category	Gene	Relevant ortholog/*C. elegans* Function/Domains
Multi-phenotypic *lin-35* Suppressors:	*isw-1*	Drosophila ISW1/chromatin remodeling, promote Ras activity/SANT, homeodomain-like, ATPase, AT-hook
	ZK1127.3	Yeast Eaf7/unknown function/novel
	F54D11.2	Yeast Muc1/unknown function/novel
	C34E10.8	Human SRMM1/unknown function/novel
	C08B11.6/*arp-1*	Yeast Arp6/unknown function/actin-like
	M03C11.3	Human ACIN1/unknown function/novel
	htz-1	Yeast Htz1/pharyngeal development/histone H2A
	sams-3	Yeast Sam1/S-adenosylmethionine synthetase, life-span/S-adenosyl methionine synthetase
synMuv Suppressors suppression	*mys-4*	Yeast NuA4 complex histone acetyltransferase Esa1/MYST histone acetyltransferase/PHD, Zinc-Finger
	gfl-1	Yeast NuA4 complex histone acetyltransferase member Yaf9/histone acetyltransferase, germline transcriptional regulation
	ekl-1	Nematode-specific/chromatin regulation/Tudor
	C17E4.6	Yeast pr-rRNA processing Nsr1/unkown function/YL1
	zhit-1	Nematode-specific/unknown function/novel
	usp-48	Yeast ubiquitin-specific protease Ubp15/unknown function/Zinc-Finger HIT-type
	rpn-10	Yeast 26 proteasome member Rpn10/proteasome functions/von Willebrand factor, ubiquitin interacting motif
	rpn-12	Yeast 26 proteasome member Rpn12/proteasome function
	T02C12.3	Mouse general transcription factor Gtfc35/unknown function/novel
	zhit-3	Yeast requirement for snoRNA accumulation Bcd1/unknown function/Zinc-finger HIT-type
	F52B11.1	Humans, Regulates Set1 histone methyltransferase complex members, CpG island

	binding/unknown function/CpG binding domain
phf-15	Yeast subunit of NuA3 histone acetyltransferase complex Nto1/unknown function/PHD, Zinc-finger PHD-type, Zinc-finger ring-type
pfd-4	Yeast subunit of prefoldin complex Gim3/unknown function/prefoldin domain
K08F4.2	Human Ras-GAP binding protein G3BP2/unknown function/RNA recognition motif
T07E3.3	Human glutathione transferase Kappa GSTK1/unknown function/Thioredoxin-like fold